

Reviewer 1: Chad Greene

General comments In this paper, Miles et al. generate observations of velocity and calving front positions of Denman Glacier, then they apply various perturbations to the geometry of a simple ice sheet model to determine what mechanisms might explain the observed behavior of the ice system. The study is elegantly designed and the manuscript is very well written.

The historical context provided by the ARGON and other early satellite photography is valuable, and I appreciate the work the authors have done to sift through the archives, in which they found a coherent and story to tell. I especially appreciate that the authors present background information in a way that sets the stage for understanding why this research was performed and what the results might mean for the future. The paper is packed with little insights such as the fascinating link between ice shelf thinning and flow direction, yet despite the density of information the text flows effortlessly. It was an enjoyable read, I learned a bit, and I recommend the paper for publication after the data and code are made publicly available.

The authors thank Chad for taking the time to review our manuscript. We appreciate his positive comments and constructive suggestions throughout the review. We respond to each point below:

Data and code sharing: This is important work, and in the future there will undoubtedly be more studies of the flow speed of Denman Glacier. Part of that work will involve reporting on changes that will have occurred since the publication of this study, and there's a good chance the authors of such a future study will want to begin by plotting velocity profiles from the 2020s on top of the results shown in Fig 3e. To allow others to build on this work, please include the coordinates and measured velocities shown in Fig 3e as supplemental material to the manuscript or upload to a data repository such as PANGAEA. Similarly, the authors have generated a wonderful calving front extent dataset shown in Fig 2b...Please share it so others may build on this work! Same goes for the Ua model code that was used to generate these results—I would love to see it after reading this paper.

Thank-you for bringing this very important point to our attention. If the manuscript is accepted we will upload all data to the UK Polar Data Centre repository, this will include: All ice-front position shapefiles, historical velocity tifs, the coordinates and measured velocities in Figure 3e and the Ua code used to generate our simulations. The source code for Ua is already available at <https://doi.org/10.5281/zenodo.3706624>

L450-464: At the end of a near-perfect manuscript in which each sentence brings new insights while setting the stage gracefully for the sentence that follows it, the final couple of paragraphs transition into a series of miscellaneous ideas that are related to, but not clearly relevant to the 2 main story of the manuscript. Each of these points could be expanded by a few sentences to help glue them to the findings of the study, but I don't think there's a need. Rather, most of the last two paragraphs could be deleted without detriment to the manuscript. I recommend simply reminding readers of the key historical behavior and/or future potential of Denman, and placing your results firmly in that context.

In the revised version we have deleted the final paragraph of the manuscript. Our conclusion now simply reminds the reader of our key results and briefly notes the potential future vulnerability of Denman Glacier.

Technical corrections

L26-27: The general sentiment of the final sentence of the abstract is reasonably supported by the analysis presented in this manuscript, but the phrase "...over the coming century" constrains the prediction a bit too tightly, because timescales of ice response are not directly discussed in this paper.

Amended to: 'that it could be poised to make a significant contribution to sea level in the near future'

L63: "...a range of remote sensing observations..." Make this sentence more clear by stating explicitly that velocity and ice front position observations are analyzed.

We have amended the text to explicitly state velocity and ice front.

L94-95: Indicate how the 1 pixel and 0.5 pixel error estimates were obtained. L113-114: Again, indicate how the error estimates were obtained.

At the request of reviewer 2 we have included a more in depth analysis of velocity uncertainties from the historical 1970s data in supplementary figure 2. This is done by comparing manually tracked rift displacement at various locations across the Denman system to computed displacement values from the Cossi-Corr algorithm. The median value of the difference between the manually tracked rift displacement and the Cossi-Corr values is $\pm 29 \text{ m yr}^{-1}$ (~ 0.5 pixels), thus justifying our estimated error.

L113-114: Again, indicate how the error estimates were obtained.

The error associated with ice-front position mapping of large Antarctic outlet glaciers has been established in several previous studies and we now make this clear in the text:

'Several previous studies (e.g. Miles et al., 2013; 2016; Lovell et al., 2017) have demonstrated that the errors associated with the manual mapping of ice-fronts from satellites with a moderate spatial resolution (10-250 m) are typically 1.5 pixels, with co-registration error accounting for 1 pixel and mapping error accounting for 0.5 pixels.'

L155-156: I don't think "accelerations" should be plural here. I recommend replacing "...with accelerations of $19 \pm 5\%$..." with "...with an overall acceleration of $19 \pm 5\%$..." Unless I've misunderstood the meaning of the sentence, in which case, please clarify.

Amended.

L246-252: I had to make this table to keep the experiments straight in my head. It may save others the same trouble to have the experiments explicitly tabulated in the manuscript.

This is an excellent suggestion and we have added a similar table (Table 1) in the revised manuscript.

L259: I think "each simulation" should be "each of the seven simulations".

Amended.

L330-331: Comparing accelerations as scalar multiples of each other is confusing, because I don't have any intuition for what it means if one thing has three times the acceleration of another thing. Actually, the sentence says "the ice accelerated approximately three times 3 faster" and if a is three times more than b, then $a=4b$, which makes the sentence even more confusing. Reword.

We have amended to text to only refer to accelerations in percent:

'Between 1972 to 1990, observations indicate that ice accelerated $26 \pm 5\%$ on the ice tongue (Fig. 3b) and $11 \pm 5\%$ at the grounding line (Fig. 3c) in comparison to more limited accelerations of $9 \pm 1\%$ and $3 \pm 2\%$, respectively, between 1990-2017'

L424: Explicitly state what “this event” is. i.e., “Thus, the next major calving event...” And if the implications are important, don’t just imply them—directly state what is implied are. i.e., “...could dictate the flow speed and direction of the...”

We have amended the text to following:

‘Thus, this calving event may have important implications for the evolution of the Denman/Shackleton system for multiple decades because it could influence both ice flow speed and direction.’

Figure 1: This figure shows bedrock topography, ice velocity, and the spatial distribution of pinning points in the Shackleton Ice Shelf. These are all valuable as context for the study, and I appreciate that the figure legend clearly states the important things that viewers should take note of. My only complaint is that each variable is plotted in a separate panel, so understanding relationships between velocity, bed topography, and pinning points requires pinballing between all three panels as a way to mentally try to bring the variables all into one figure. Reconstituting the three variables is made more difficult by the fact that each panel shows different spatial extents, and at different scales. I recommend experimenting with transparency, vectors, or contours to show all three variables on one plot. That would also allow more detail, as a single panel could be enlarged to fill the entire width of the page. For example, something like the following would be a way to show ice velocity in the context of surface features and the bed topography that ties Denman Glacier to the ASB:

We have revised figure 1 so that all three variables (velocity, bed topography and pinning points) are displayed on the same figure. On the basis of some of the other reviewer comments we also include a bed profile subplot taken over the Denman grounding line.

Figure 2: As a logical sequence, I’d also put panel b before panel a, because currently panel b shows the direct observations and then panel a shows a quantified version of the observations. I’m also having difficulty understanding where panels c-f are in relation to panel b. There are no recognizable reference points in any of the images, so it’s difficult to place them in space. I would typically assume that the image orientation remains constant across all panels, but the spatial extent and even the spatial scale is different in each panel, so everything is in question.

It’s also tempting to assume panels c-f depict a sequence of events, but they are presented out of chronological order, so there’s an extra little bit of mental bookkeeping that viewers must do to reconstruct what has happened to this glacier tongue since 1962.

If it makes sense to do so, I’d like to see the spatial extents of panels c-f remain constant across all panels, so it will be easy to follow changes over time. I suspect the entire figure would be easier to digest if the panels were rearranged, and if the times of panels c-f were marked directly on the ice front position time series. Something along these lines feels much more intuitive to me:

Or perhaps the time series plot would fit best below the calving-front map, but however you do it, I think the sequence of the panels is important for understanding what story is being told by the figure, and drawing direct connections between all the panels (such as by labeling the times of panels c-f directly on the time series) will help viewers see how the information is all related.

Also, more can be done in the caption to help readers understand the connection between ice front position and ice morphology. This could be just a sentence or two, but just something to help viewers see why R1 through R7 are labeled.

In the revised figure with have added an additional panel (a) which provides a wider picture and highlight the location of the subsequent sub plots. We have also added a consistent reference grid to

all panels to provide a reference point on both the size and location of each figure. We have also added the times of the panels (d-g) to the ice-front time series.

We have also added more detail to the figure caption and included more detail on the importance of R1-R7:

‘Figure 2: a) Overview of the Denman ice tongue with the coloured boxes indicating the locations of c-g. b) Reconstructed calving cycle of Denman Glacier 1940-2018. c) Examples of ice-front mapping 1962-2018. Note the change in angle of the ice shelf between its present (light blue – dark blue lines) and previous (pink-red lines) calving cycle. d) ARGON image of a large tabular iceberg in 1962 which likely calved from Denman at some point in the 1940s. e) Landsat-1 image of the Denman ice tongue in 1972, note the pattern of rifting labelled R1-R7. f) Landsat-4 image of a large tabular iceberg which calved from Denman in 1984. Note the rifting pattern and the absence of R7, meaning R7 likely propagated during its calving event in 1984. g) Landsat-8 image of the Denman ice tongue. Note the absence of rifting.’

Figure 3: State which grounding line dataset is being shown here. Partly to give credit to the data producers, but also because InSAR and break-in-slope grounding lines don’t agree here, and knowing which GL is plotted would help readers visually identify where certain features are relative to a particular GL

The grounding line product used in Figure 3 is from Depoorter et al. (2013). We use this product for display purposes on the figure because it shows a clear and continuous grounding line across the study area. We have added the citation to the figure caption.

Figure 5: The mental ledger keeping required to interpret this figure is not terribly onerous, but it involves more steps than are necessary. For example, if I want to know what’s being depicted in panel g, I must go to the legend in the bottom left, where I see g corresponds to E6, then I find E6 in panel i, and then I say, “okay, E6 falls closer to a dashed line than most of the other dots do.” And then I get curious about the outlier dot corresponding to E4 on the x axis. “I wonder what that is,” I think, and so I repeat the process backward, going to the legend in the lower left of the figure to find that E4 corresponds to panel e, so then I look at panel e and I see a mostly blank white panel. At no point in that process is there any indication of what any of 7 these letters and numbers mean, because the figure has been stripped of all links to physical processes.

I recommend eliminating the legend from the bottom left and simply labeling “E1: ice shelf thinning,” “E2: grounding line retreat,” etc., directly on panels a-h, either as titles outside the plot or in the empty space in the bottom of each panel. That would also free up the text of the figure caption to focus on physical processes, rather than bookkeeping.

In the text caption, hammer home the main point by stating that E7 most closely matches observed velocities, suggesting that ice shelf thinning, grounding line retreat, and unpinning from Chugunov Island have all occurred since 1972.

Panel c shows the effects of grounding line retreat, but grounding line retreat itself is not shown. It’s hard to gauge spatial scales here, but would a 10 km retreat be visible at this scale? If so, show both the 1972 and 2009 grounding lines.

Panel e shows the effects of unpinning from Chugunov Island. It would be helpful to label Chugunov Island directly on that panel.

I appreciate that panel i puts most meaningful region of velocities of each experiment in context with each other, while also showing the observed 1972 and 2009 velocities, but the panel comes up short in communicating the main point. It's relatively innocuous, so keep the panel if it feels important, but know that it adds a layer of complication to interpreting the figure as a whole. If you'd like to keep it, I recommend including Box D velocities from panel a as a data point. That would make it more clear how E4 got so out of line relative to the others. If you decide to eliminate panel i, the ice speed values could simply be printed next to Box D in their respective panels and/or included as a column in the table I recommended above.

I find myself leaning in close and squinting to see the details around the grounding line. Then I zoom the pdf to 300% and realize the problem isn't my eyesight, but the coarse resolution of the graphics. I recommend recreating the figure at higher resolution (If it's Matlab, try `export_fig myfigure.png -r600` for 600 dpi) and enlarging the figure to fill the full width of the page so readers can see the beautiful details that are surely present in this data.

We have added a text description of the experiment number and the perturbations forced in each panel of the figure to prevent the reader having to constantly flick between the caption and the figure. We have also labelled Chugunov Island on the appropriate figures. The scale is too coarse to the differing grounding line positions to be visible, but we do note that a close up version of the grounding line positions used in the simulations are in Fig S3. We have decided to keep panel I, which shows the velocities at box D to be consistent with the time series of speed change in Figure 3. We have also increased the resolution of the figure so more detail can be observed when zooming in and amended the figure caption.

Reviewer 2

In this manuscript by Miles et al., the authors explore the connection between surface ice velocity acceleration and calving events for Denman Glacier, East Antarctica. Particularly, to explore this connection, the authors apply several tools ranging from remote sensing observations to ice sheet modelling to grasp which mechanisms might explain the acceleration and ground line retreat of Denman Glacier.

The manuscript is very well written and flows quite smoothly in the description of the methods and the used ice sheet models. As a remote sensing expert, I really liked the contribution brought by the historical remote sensing data, which are generally very difficult to find. The main hassle for me was going through all the figure. The absence of system coordinates makes very difficult to go from one figure to the other and make connections and comparisons between the figure. Therefore, I recommend the paper to be published after major revisions. In the following, some additional comments.

We thank the reviewer for both the positive comments detailed above and for the constructive suggestions suggested below. We respond to each point detailed below.

Line 11, identifying Denman glacier as the largest is really vague. For a reader, it would be nice to specify that e.g. this glacier is the largest contributor to sea level rise in East Antarctica (after Totten Glacier)

We have amended the sentence to state that Denman is the largest contributor to sea level rise in East Antarctica after Totten Glacier.

2. One of the major statements of the paper is that to explain the acceleration pattern of Denman Glacier it is required to have a combination of grounding line retreat, changes in ice shelf thickness and unpinning of ice from Chugonov Island (lines 331-334). I am wondering if the unpinning of Chugonov Island comes from observations. Did the authors observe the unpinning in their data?

We do observe the unpinning of Denman's ice tongue from Chugonov Island. This is shown in Figure 4d & e and is described in the results section 3.3: 'Lateral migration of Denman's ice tongue':

'In 1974, the ice tongue was intensely shearing against Chugonov Island, as indicated by the heavily damaged shear margins (Fig. 4d). However, by 2002 the ice tongue made substantially less contact with Chugonov Island because this section of the ice tongue migrated westwards (Fig. 4d, e)'

3. Line 94-95 and line 109-112. Have the authors quantitatively determined the uncertainty of surface ice velocity obtained from historical data? Instead of providing a ball park number, it would be nice to have a section in the supplementary describing how they quantified this uncertainty.

We now include an additional figure in the supplement (Fig. S2) detailing the quantification of the velocity error for the historical imagery. This is done by comparing manually tracked rift displacement at various locations across the Denman system to computed displacement values from the Cossi-Corr algorithm. The median value of the difference between the manually tracked rift displacement and the Cossi-Corr values is $\pm 29 \text{ m yr}^{-1}$ (~ 0.5 pixels), thus justifying our estimated error.

4. To my understanding, to perform their analysis the authors have used the Measure grounding line product for Denman. Do you know to which sensor and which year this grounding line belongs to? Also, have the authors tried to include more recent grounding line products?

We use the grounding line position from the BedMachine (v1) dataset, which in turn matches the grounding line position of the MEaSUREs dataset. The grounding line in the MEaSUREs dataset was derived from the ERS sensor in 1996. More recent grounding line products (~2017) over Denman have been made as of April 2020 (Brancato et al., 2020). We have not tried to include this more recent grounding line data into our models in order to retain consistency with the ice thickness calculated in the BedMachine product.

5. I find really difficult to go through all the model experiments that the authors have performed. Is there a way to visually summarize them in the manuscript, e.g. using a table?

We appreciate the multitude of modelling experiments is somewhat challenging to summarize in text, so we now include a table which visually summarizes the seven experiments (Table 1).

6. To explain the acceleration of Denman glacier, in Section 5.2 the authors discuss whether this is driven by warm water intrusion (e.g. ice-ocean interactions) or calving events. I find this section a bit confusing especially because it introduces a lot of elements which have not previously discussed in the manuscript. Do the authors simulate with their ice model the effect of the ice-ocean interaction? Also, does the model take into account the effect of basal melt of Denman ice shelf?

In our numerical modelling experiments we perturb both grounding line position and ice shelf thickness. These perturbations are extrapolated from modern observations of change (Ice shelf thickness; Paolo et al.; Grounding line migration; Brancato et al., 2020). Because both grounding line position and ice shelf thickness are sensitive to ice-ocean interaction, our model does indirectly simulate possible long-term effects of ice-ocean interaction.

7. As a general comment, ALL figures need to have coordinates grid. For me it was extremely difficult to move from one

We have added coordinate grids to all figures.

8. I find the colorbar in figure 1-a to be confusing. Maybe all areas with an elevation over 0 should be marked with the same color, e.g. white.

9. Without coordinates is a bit difficult to link Fig.1b and Fig.1c. I would recommend to highlight the area in Fig.1c using a box in Fig.1b

Point 8 & 9: In response to the comments from all three reviewers we have made a new Figure 1. This revised figure 1 has reference coordinates and only highlights regions with a bed elevation below zero.

10. Date of used Landsat images and acknowledgement for the used Landsat product should be included in the figure caption. Please, see USGS website for getting the proper data citation.

We have added the dates and acknowledgement for the used Landsat products in the figure captions.

11. For Fig.2, each panel focus on a different area of the ice shelf. I would recommend to have a bigger picture of the ice shelf on the side and try to help the reader understand on which areas you are focusing/zooming on. Please, include latitude and longitude (or polar stereographic) coordinates for each figure.

We have amended figure 2 to include a reference image of the wider ice shelf (a) with boxes representing the location of each sub figure. We have also included polar stereographic coordinates on each image for reference.

Reviewer 3

In this manuscript, Miles et al reconstructed the migration of ice front and the evolution of the velocity field of Denman Glacier, Aurora subglacial basin, East Antarctica based on satellite images from 1962 to 2018. The ice sheet model Ua is then implemented to study the potential drivers of the widespread acceleration of Denman glacier between 1972 and 2009.

The manuscript is well written and easy to follow. Reconstruction of historical evolution of ice flow as well as the calving events is valuable for modellers to verify and improve the physical processes and parameterizations in the ice sheet models. While the observation work is fascinating, I find the numerical modeling experiments not enough to support the conclusions. The authors conclude that grounding line retreat, ice tongue thinning and unpinning from the pinning point are necessary to rebuild the acceleration over the glacier, and therefore emphasize the impact of ocean warming and calving events to the dynamics of Denman glacier. The three experiments are thinning the ice shelf, adjusting the bedrock elevation near the grounding line, and altering the bedrock elevation of the pinning point. Changing the bedrock elevation to mimic the same unpinning seen by the ice fractures is very tricky, since it affects the entire ice geometry for the wrong reasons. I think the ice sheet model Ua is capable to simulate what you want to investigate, but I suggest adaptations of the simulations (see specific comments). Therefore, I suggest a major change of the manuscript for the simulation sections.

We thank the reviewer for taking the time to comment on our manuscript and for the positive comments detailed above. We address the reviewers concerns on our simulations below:

Specific comments

Line 15: It's mentioned several times in the manuscript the potential instability due to the retrograde slope. I think it could help the readers to understand the configuration better if the authors show in one of the figures (e.g. Fig. 1) a transect along the flow line to show the geometry.

We now include a transect along the flow line in the subpanel in Figure 1 to show the retrograde slope.

Line 30: Is 'Wilkes Land' here and also in Line 49 the same region as 'Aurora Subglacial Basin'? If so, use one of them to avoid confusion.

Wilkes Land is the geographical region, whereas the Aurora Subglacial Basin is the subglacial basin within Wilkes Land. We have amended the text to avoid confusion:

'This has raised concerns about the future stability of some major outlet glaciers along the Wilkes Land coastline that drain the Aurora Subglacial Basin (ASB)'

Line 68: mention also the conclusions section.

We have added reference to the conclusion in the text.

Line 127-129: The authors predicted that calving event is unlikely due to the absence of any significant rifting or structural damage. The context of calving is missing in the introduction section, such as what could be the earlier indicators of calving events and how do we predict calving.

We appreciate the reviewers point here. However, we note that the concept of the prediction of Denman's next calving event is only a very small part of the manuscript. We feel that adding

background information on the early indicators of calving events in the introduction would distract from the manuscripts main aim – to explore the drivers of Denman’s acceleration since 1972.

Line 139-140: Could you make the scales of subplots of Figure 2 consistent to clearly show the information?

This is a good suggestion. We have revised Figure 2 to make the scales of the subplots in figure 2 consistent.

Line 147-148: Are the rifts a indicator of calving events? Can you discuss more about the formation and development of the rifts? From Figure 2 it’s hard for me to see.

We hypothesize that the rifting observed on the Denman ice tongue in the 1970s was important in Denman’s calving in 1984. This is because an analysis of the rift patterns on the ice tongue in 1974 and on the subsequent grounded iceberg in 1990 show that the iceberg calved from Rift 7 (See Fig. 2e,f). However, further discussion on the formation and development of the rifts is tricky. This is because we only have satellite imagery available in 1972 and 1974, the next full available image over the Denman ice tongue is not until 1989. Therefore, commenting further on the formation and development of these rifts is very difficult without a greater density of observations.

We have clarified this in the text:

‘The rifts periodically form ~10 km inland of Chugunov Island (Fig. 2e), on the western section of the ice tongue, before being advected down-flow. But a more detailed analysis of how the rifts form is not possible because of the limited available satellite imagery in the 1970s and 80s.’

Line 151: ‘Fid. 2d’ → ‘Fig. 2d’

Amended.

Line 159-161: In year 1984 there is a calving event. Do you think that could be one of the reasons that the speed-up is much higher between 1972-74 and 1989 while between 1989 and 2016-17 is slower?

This is an interesting point. If the ice calved in 1984 provided buttressing, a speed up after the calving event would be expected. However, we note that changes in ice shelf extent have not been a dominant driver in the longer-term speed up of Denman. This is because the ice front was further advanced in 2018 than it was in 1972, but ice at Denman’s grounding line is flowing 17% faster in 2018 than it did in 1972. We think the main importance of the calving event in the longer-term evolution of Denman, is that it enabled ice to re-advance at a different angle and make less contact the pinning point.

In order to test the direct importance of the calving event on ice velocity we would ideally need satellite image pairs either side of the event, but unfortunately such imagery is not available. In the absence of satellite imagery, we could simulate the calving event by altering the ice-front position in Úa. We agree that this would be an interesting experiment, but we note that we already show seven numerical modelling experiment and that adding a further perturbation may add further complication to an already busy manuscript. Indeed, we note our justification for choosing to compare ice geometries in 1972 and 2009 is that observations show that ice front position was similar in each time period.

We have added further clarification in the text at line 225:

‘We chose 2009 for this baseline setup, because the calving front is in approximately the same position as in 1972 when our glacier observations start, thus ruling out any acceleration is response to a change in ice-front extent’

Line 180-182: Could you have another layer of ice flow magnitude and directions (arrows like Figure 5) on top to show the divergence of the ice flow?

We have added the MEASUREs velocity magnitude and direction to the overview figure (4a). We do not add the change in direction in flow due to the patchy nature of the data in the 1970s.

Line 202-204: 'Ice rheology is assumed to...' → 'The relationship between creep and stress is assumed to...'

Amended.

Section 4.1: Modelling work is done to understand the acceleration/slowing down of the observed ice flow. Therefore, I think it's essential to at least show the momentum equations implemented by the ice sheet model, where the readers C4 TCD Interactive comment Printer-friendly version Discussion paper could clearly see how ice geometry, basal sliding and ice rheology influence the velocity field.

We have added the following to line 192:

\dot{u} is used to solve the equations of the shallow-ice stream or 'shelfy-stream' 193 approximation, (SSA, Cuffey & Paterson, 2010). This can be expressed for one horizontal dimension as :

$$2\partial_x \left(A^{-1/n} h (\partial_x u)^{1/n} \right) - \rho G - C^{-1/m} u^{1/m} = \rho g h \partial_x s + \frac{1}{2} g h^2 \partial_x \rho$$

Where A is the rate factor with its corresponding stress factor n , h is the vertical ice thickness, G is a grounding/flotation mask (1 for grounded ice, 0 for floating ice), C is the basal slipperiness with its corresponding stress exponent, m , ρ is the density of ice and g is the acceleration due to gravity.

Section 4.2: The experiments are diagnostic based on the ice geometry from 2009 and the reconstructed ice geometry from 1972, is that right? This should be clarified.

For clarification, Line 223 has been changed to:

"To ascertain the most likely causes of the observed acceleration for Denman ice shelf we start from a baseline set-up representing the ice shelf in 2009 where both ice geometry and velocity are well known and compare to diagnostic simulations of reconstructed 1972 ice geometry"

Experiment (i): The authors modified the ice-shelf thickness with an annual rate. How about the grounded ice upstream from the ice shelf? Are they kept the same between the two simulation years? Will it cause a dramatic thickness change near the grounding line in 1972? Or is there an interpolation done? Please describe your method. Could you show the geometry difference between the two simulations somewhere in the figures?

The thinning is applied only to fully floating nodes with grounded ice kept constant between simulations in a similar methodology used in Gudmundsson et al. 2019. As only fully floating are modified in this way, the thickness at the grounding line itself remains unmodified between the two simulations. Supplementary Figure 4 shows the thickness change applied, with a ~10 m thickening in the vicinity of the grounding line. The paragraph beginning line 235 has been changed to the following to include these additional clarifications.

“To represent ice shelf thinning since 1972, we take the mean annual rate of ice-thickness change from an 1994–2012 ice-shelf thickness change dataset (Paolo et. al., 2015) and scale it up to represent the total thickness change over the 37 years between 1972 and 2009, assuming that the 1994–2012 mean annual rate remains constant during this period. This thickness change is then applied to the 2009 ice geometry, modifying it to better represent the estimated 1972 ice thickness distribution of the Shackleton Ice Shelf, Denman ice tongue and Scott Glacier. Similar to the methodology of Gudmundsson et al. 2019, we only apply this thickness change to fully floating nodes, with no change of ice thickness for grounded ice and ice directly over the grounding line. The total thickness change applied is shown in Supplementary Figure 4. We refer to this perturbation as ‘ice shelf thinning’ because the majority of the floating portions of Denman’s ice tongue and Shackleton Ice Shelf have thinned since 1994, although some sections of Scott Glacier have actually thickened near its calving front (Fig. S4).”

Experiment (ii): I think it’s not appropriate to call this experiment ‘grounding line retreat’, because grounding line retreat is impossible without ice geometry change. This experiment adjust the bedrock to have grounding line at a different location. How much uplifting is needed? Normally the bedrock won’t have significant change in short term. The difference of velocity comes from additional basal friction in the uplifted region. This experiment actually shows the sensitivity of velocity field to the basal sliding near the grounding line.

Our methodology is not designed to represent any real earth processes such as isostatic rebound but is instead intended to show the instantaneous effect of a grounding line perturbation on ice velocity with the minimum possible bias to the existing ice velocity field. Directly modifying the ice geometry at the grounding line will have a noticeable effect on the regional ice velocity field due to conservation of flux in addition to any changes arising from the shift in grounding line position, and so we instead raise the bedrock to force the models grounding line to be at a given location. The paragraph starting line 247 has been modified to clarify this:

“In the Úa ice model, the grounding line position is not explicitly defined by the user but is instead a direct result of ice thickness, bedrock depth and the relative densities of ice and sea water. As such, the two ways to perturb a given grounding line are to either modify the ice thickness or the bedrock depth. Modifying the bedrock depth is the less disruptive approach because the resulting effect upon velocity is not biased by an imposed change in ice thickness at the grounding line effecting the regional ice velocity field due to flux conservation, in addition to that caused by shifting the grounding line. Note that raising the bedrock to meet the underside of the ice shelf in this way is not a representation of any real earth processes, it is merely forcing the model to have the grounding line in a particular location, that than enables a diagnostic simulation. To represent grounding line retreat since 1972 we advanced Denman’s grounding line from its position in the 2009 baseline set-up by 10 km to a possible 1972 position. This is achieved via raising the bedrock approximately ~20-30 m in the area shown in Fig. S4. We justify a 10 km retreat since 1972 based on the rate of grounding-line retreat observed between 1996 and 2017 (~5km; Brancato et al., 2020). For the newly grounded area, values of the bed slipperiness, C , are not generated in our model inversion, we therefore prescribe nearest-neighbour values to those at the grounding line in the model inversion.”

Experiment (iii): It’s mentioned in the abstract and the discussion section that the unpinning of ice from Chugunov Island is due to the calving event. From Fig. 4d, e, and also mentioned in the results

section, the ice around Chugunov Island might be heavily damaged, leading to unpinning/debuttressing. The calving effect and the damage effect could be simulated by changing the ice front or modify the rate factor 'A'. Why did the authors decide to evaluate the unpinning effect by changing bedrock? Furthermore, how much do you need to change to have the proper unpinning effect?

We agree with the reviewers point that the unpinning from Chugunov Island could be investigated by modifying the rate factor 'A', in addition to the regrounding experiment shown. Due to the limited information about past conditions of ice geometry and properties available to us, any attempt to simulate past conditions will have to some extent rely upon assumptions. We would argue that the assumptions made for the regrounding of the ice at Chugunov Island are more justifiable than those that would be required for an investigation into the rate factor, 'A'. Performing new model inversions using 1972 velocities and ice geometry would be the ideal way to investigate this. However, as the 1972 velocities are relatively patchy and the 1972 ice geometry itself an unknown under investigation it would be impossible to separate out the effect of the damaged ice on both velocity and rate factor from that arising from ice geometry change. The assumptions needed to investigate the effect of regrounding the ice at Chugunov island are easier to justify. Raising the bedrock by ~30m is enough to ground ice along the edge of the model domain and we have assumed basal slipperiness, C, is the same as that located near the grounding line. The paragraph beginning line 263 has been modified to further articulate our reasoning:

"To represent the pinning of Denman's ice tongue against Chugunov Island in the 1972 observations (e.g. Fig. 4d, e), we artificially raise a small area of bedrock on the western edge of Chugunov Island (Fig. S3). Bed slipperiness was set to a value comparable to that immediately upstream of the grounding line. Note that, although past observations suggest that the ice in front of Chugunov Island has been damaged, possibly having an effect on its rate factor, A, we have decided to limit our investigation to the effect of pinning the ice on Chugunov Island without changing rate factor. To properly investigate the possible change in past rate factor we would need less spatially patchy 1972 velocities as well as an accurate understanding of past ice geometry (itself an unknown under investigation) to perform a model inversion for 1972 conditions."

Line 267: E1 is Fig. 5b, not Fig. 5a.

Amended

Line 281: 'experiment 5' → 'experiment E5' or 'E5' same for the other experiments there after.

Amended

Line 286-288: Can you explain why the acceleration on the ice shelf is much higher than the grounding line (Fig. 5a) but all simulations show the opposite pattern?

For most of these simulations a direct comparison can be potentially misleading as we are applying the perturbations in isolation of one another to investigate the general pattern of change in velocity association with each individual perturbation. For example, the isolated un-pinning experiment (Fig. 5e) clearly shows that unpinning from Chugunov Island has a negligible effect on grounding line velocity. The difference from observations for most of these simulations is probably due to the simulations not only omitting a perturbation in ice geometry but also the interactions between different types of perturbation. For the simulation which includes all three perturbations (Fig. 5h) the difference from observations is noticeably less than in the isolated perturbations, and remaining differences can most likely be attributed to the uncertainties in the perturbations applied (eg.,

assuming the thickness change over the 37 years is the same as the annual scaled mean change between 1994–2012).

Line 361: 'E3; Fig. 5e' → 'E3; Fig. 5d'?

Amended

Line 362: 'E4; Fig.5d' → 'Fig. 5a'?

Amended

Line 367: 'E4; Fig. 5d' → 'E4; Fig. 5e'?

Amended

Line 379-381: Could the authors add the simulation of calving event by simply change the ice front position and evaluate its influence on ice velocity?

Our observations show that changes in ice-front extent was unlikely to have driven the long-term acceleration of Denman. This is because that Denman's ice-front is currently further advanced than it was in 1972, but we still observe a 17% acceleration in flow over the grounding line. Therefore, we do not simulate the impact of the calving event by changing the ice-front position because our observations demonstrate that this is not an important contributor to the long-term acceleration of Denman

In our description of the perturbation experiments we clarify our rationale for not simulating the change in ice-front position (Line 225):

'We chose 2009 for this baseline setup, because the calving front is in approximately the same position as in 1972 when our glacier observations start, thus ruling out any acceleration is response to a change in ice-front extent'

Line 433: 'hydrofracturing' → 'hydrofracturing.'

Amended.

Line 447: Morlighem et al., 2019 is not in the reference list.

Amended. The citation in the main text should read 'Morlighem et al., 2020' – we have corrected throughout.

Figure 1: Could the authors add the transection of the geometry along a flow line to clearly show the retrograde bed? Maybe show the perturbation of bedrock in experiment (ii) in the same plot. Point out the position of Chugunov Island.

This is a good suggestion and we have added a transect of the bedrock elevation along the flow line in a subplot to show the retrograde slope.

Figure 2: The subfigures are oriented in different ways, and with different scales, making it hard to compare the size of ice bergs, the development of rifts and so on. Could you have a zoom out subfigure like Figure 1b and put the boxes on top to show the zoom in area of the subfigures?

We have revised Figure 2 to include a zoom out subfigure with boxes indicating the location of the other subpanels. We have also added reference coordinates to all panels and made the scales consistent to enable an easier comparison of the icebergs and rifts.

Figure 4: Could you add a layer of velocity (magnitude and direction) on top of the satellite images to show the change of ice flow? That will make the figure more self-explanatory.

We have added velocity magnitude and direction to the overview figure (4a). We do not add the change in direction in flow due to the patchy nature of the data in the 1970s.

Figure 5: I think there should be a grounding line contour at the pinning point Chugunov Island.

We have added a grounding line contour around Chugunov Island on the appropriate panels.

Figure S2: Could you have a subfigure of simulated velocity? And also please show the location of the grounding line.

Figure S2 has had the recommended changes made.

Recent acceleration of Denman Glacier (1972-2017), East Antarctica, driven by grounding line retreat and changes in ice tongue configuration.

Bertie W.J. Miles^{1*}, Jim R. Jordan², Chris R. Stokes¹, Stewart S.R. Jamieson¹, G. Hilmar Gudmundsson², Adrian Jenkins²

¹Department of Geography, Durham University, Durham, DH1 3LE, UK

²Department of Geography and Environmental Sciences, Northumbria University, Newcastle upon Tyne, NE1 8ST, UK

*Correspondence to: a.w.j.miles@durham.ac.uk

Abstract: After Totten, Denman Glacier is the largest contributor to sea level rise in East Antarctica. Denman's catchment contains an ice volume equivalent to 1.5 m of global sea-level and sits in the Aurora Subglacial Basin (ASB). Geological evidence of this basin's sensitivity to past warm periods, combined with recent observations showing that Denman's ice speed is accelerating, and its grounding line is retreating along a retrograde slope, have raised the prospect that its contributions to sea-level rise could accelerate. In this study, we produce the first long-term (~ 50 years) record of past glacier behaviour (ice flow speed, ice tongue structure, and calving) and combine these observations with numerical modelling to explore the likely drivers of its recent change. We find a spatially widespread acceleration of the Denman system since the 1970s across both its grounded ($17 \pm 4\%$ acceleration; 1972-2017) and floating portions ($36 \pm 5\%$ acceleration; 1972-2017). Our numerical modelling experiments show that a combination of grounding line retreat, ice tongue thinning and the unpinning of Denman's ice tongue from a pinning point following its last major calving event are required to simulate an acceleration comparable with observations. Given its bed topography and the geological evidence that Denman Glacier has retreated substantially in the past, its recent grounding line retreat and ice flow acceleration suggest that it could be poised to make a significant contribution to sea level in the near future.

1. Introduction

Over the past two decades, outlet glaciers along the coastline of Wilkes Land, East Antarctica, have been thinning (Pritchard et al., 2009; Flament and Remy, 2012; Helm et al., 2014;

Schröder et al., 2018), losing mass (King et al., 2012; Gardner et al., 2018; Shen et al., 2018; Rignot et al., 2019) and retreating (Miles et al., 2013; Miles et al., 2016). This has raised concerns about the future stability of some major outlet glaciers along the Wilkes Land coastline that drain the Aurora Subglacial Basin (ASB), particularly Totten, Denman, Moscow University and Vanderford Glaciers. This is because their present day grounding lines are close to deep retrograde slopes (Morlighem et al., 2020), meaning there is clear potential for marine ice sheet instability and future rapid mass loss (Weertman, 1974; Schoof, 2007), unless ice shelves provide a sufficient buttressing effect (Gudmundsson, 2013). Geological evidence suggests that there may have been substantial retreat of the ice margin in the ASB during the warm interglacials of the Pliocene (Williams et al., 2010; Young et al., 2011; Aitken et al., 2016; Scherer et al., 2016), which potentially resulted in global mean sea level contributions of up to 2 m from the ASB (Aitken et al., 2016). This is important because these warm periods of the Pliocene may represent our best analogue for climate by the middle of this century under unmitigated emission trajectories (Burke et al., 2018). Indeed, numerical models now predict future sea level contributions from the outlet glaciers which drain the ASB over the coming decades to centuries (Golledge et al., 2015; Ritz et al., 2015; DeConto and Pollard, 2016), but large uncertainties exist over the magnitude and rates of any future sea level contributions.

At present, most studies in Wilkes Land have focused on Totten Glacier which is losing mass (Li et al., 2016; Mohajerani et al., 2019) in association with grounding line retreat (Li et al., 2015). This has been attributed to wind-forced warm Modified Circumpolar Deep Water accessing the cavity below Totten Ice Shelf (Greenbaum et al., 2015; Rintoul et al., 2016; Greene et al., 2017). However, given our most recent understanding of bedrock topography in Wilkes Land, Denman Glacier (Fig. 1) provides the most direct pathway to the deep interior of the ASB (Gasson et al., 2015; Brancato et al., 2020; Morlighem et al., 2020). Moreover, a recent mass balance estimate (Rignot et al., 2019) has shown that, between 1979 and 2017, Denman Glacier's catchment may have lost an amount of ice (190 Gt) broadly comparable with Totten Glacier (236 Gt). There have also been several reports of inland thinning of Denman's fast-flowing trunk (Flament and Remy, 2012; Helm et al., 2014; Young et al., 2015; Schröder et al., 2018) and its grounding line has retreated over the past 20 years (Brancato et al., 2020). However, unlike Totten and other large glaciers which drain marine basins in Antarctica, there has been no detailed study analysing any changes in its calving cycle, velocity or ice tongue structure. This study reports on remote sensed observations of ice-front position and velocity change from 1962 to 2018 and then brings these observations together with

numerical modelling to explore the possible drivers of Denman's long-term behaviour. The following section outlines the methods (section 2) used to generate the remote sensing observations (section 3) and we then outline the numerical modelling experiments (section 4) that were motivated by these observations, followed by the discussion (section 5) and conclusion (section 6).

2. Methods

2.1 Ice front and calving cycle reconstruction

We use a combination of imagery from the ARGON (1962), Landsat-1 (1972-74), Landsat 4-5 (1989-1991), RADARSAT (1997) and Landsat 7-8 (2000-2018) satellites to create a time series of ice-front position change from 1962-2018. Suitable cloud-free Landsat imagery was first selected using the Google Earth Engine Digitisation Tool (Lea, 2018). Changes in ice-front position were calculated using the box method, which uses an open ended polygon to take into account any uneven changes along the ice-front (Moon and Joughin, 2008). To supplement the large gap in the satellite archive between 1974 and 1989 we use the RESURS KATE-200 space-acquired photography from September 1984. This imagery is hosted by the Australian Antarctic Data Centre, and whilst we could not access the full resolution image, the preview image was sufficient to determine the approximate location of the ice-front and confirm that a major calving event took place shortly before the image was acquired (Fig. S1).

2.2 Velocity

Maps of glacier velocity between 1972 and 2002 were created using the COSI-Corr (CO-registration of Optically Sensed Images and Correlation) feature-tracking software (Leprince et al., 2007; Scherler et al., 2008). This requires pairs of cloud-free images where surface features can be identified in both images. We found three suitable image pairs from the older satellite data: Nov 1972 – Feb 1974, Feb 1989 – Nov 1989, and Nov 2001 – Dec 2002. We used a window size of 128 x 128 pixels, before projecting velocities onto a WGS 84 grid at a pixel spacing of 1 km.

To reduce noise, we removed all pixels where ice speed was greater than $\pm 50\%$ the MEaSURES ice velocity product (Rignot et al., 2011b), and all pixels where velocity was $< 250 \text{ m yr}^{-1}$. Errors

are estimated as the sum of the co-registration error (estimated at 1 pixel) and the error in surface displacement (estimated at 0.5 pixels) which is quantified from comparing computed velocity values to estimates derived from the manual tracking of rifts in the historical imagery (Fig. S2). This resulted in total errors ranging from 20 to 73 m yr⁻¹. Annual estimates of ice speed between 2005-2006 and 2016-2017 were taken from the annual MEaSUREs mosaics (Mouginot et al., 2017). These products are available at a 1 km spatial resolution and are created from the stacking of multiple velocity fields from a variety of sensors between July and June in the following year. To produce the ice speed time-series, we extracted the mean value of all pixels within a defined box 10 km behind Denman's grounding line (see Fig. 3). To eliminate any potential bias from missing pixels, we placed boxes in locations where all pixels were present at each time step.

We also estimated changes in the rate of ice-front advance between 1962 and 2018. This is possible because inspection of the imagery reveals that there has been only one major calving event at Denman during this time period because the shape of its ice front remained largely unchanged throughout the observation period. Similar methods have been used elsewhere on ice shelves which have stable ice fronts e.g. Cook East Ice Shelf (Miles et al., 2018). This has the benefit of acting as an independent cross-check on velocities close to the front of the ice tongue that were derived from feature tracking. The ice-front advance rate was calculated by dividing ice-front position change by the number of days between image pairs. Previous studies (e.g. Miles et al., 2013; 2016; Lovell et al., 2017) have demonstrated that the errors associated with the manual mapping of ice-fronts from satellites with a moderate spatial resolution (10-250 m) are typically 1.5 pixels, with co-registration error accounting for 1 pixel and mapping error accounting for 0.5 pixels. This results in ice-front advance rate errors ranging from 6 to 73 m yr⁻¹. The general pattern of ice-front advance rates through time is in close agreement with feature tracking-derived changes in velocity over the same time period.

3. Results

3.1 Ice tongue calving cycles and structure

Throughout our observational record (1962 - 2018) Denman Glacier underwent only one major calving event, in 1984, which resulted in the formation of a large 54 km long (1,800 km²) tabular iceberg (Fig. 2). Since this calving event in 1984 the ice-front has re-advanced 60 km and there have been no further major calving events (Fig. 2b, c), as indicated by minimal

changes to the geometry of its 35 km wide ice front. As of November 2018, Denman Glacier's ice-front was approximately 6 km further advanced than its estimated calving front position immediately prior to the major calving event in 1984 (Fig. 2b, c). However, given the absence of any significant rifting or structural damage, a calving event in the next few years is unlikely. This suggests the next calving event at Denman will take place from a substantially more advanced position (>10 km) than its last observed event in 1984.

Following the production of the large tabular iceberg from Denman Glacier in 1984, it drifted ~60 km northwards before grounding on the sea floor (Fig. 2f), and remained near stationary for 20 years before breaking up and dispersing in 2004. Historical observations of sporadic appearances of a large tabular iceberg in this location in 1840 (Cassin and Wilkes, 1858) and 1914 (Mawson, 1915), but not in 1931 (Mawson, 1932), suggest that these low-frequency, high-magnitude calving events are typical of the long-term behaviour of Denman Glacier. In 1962, our observations indicate a similar large tabular iceberg was present at the same location (Fig. 2d) and, through extrapolation of the ice-front advance rate between 1962 and 1974 (Fig. 2b), we estimate that this iceberg was produced at some point in the mid-1940s. However, the iceberg observed in 1962 (~2,700 km²) was approximately 50% larger in area than the iceberg produced in 1984 (~1,700 km²), and 35% longer (73 km versus 54 km). Thus, whilst Denman's next calving event will take place from a substantially more advanced position than it did in 1984, it may not be unusual in the context of the longer-term behaviour of Denman Glacier (Fig. 2b).

There are clear differences in the structure of Denman Glacier between successive calving cycles. In all available satellite imagery between the 1940s and the calving event in 1984 (e.g. 1962, 1972 and 1974) an increasing number of rifts (labelled R1 to R7) were observed on its ice tongue throughout this time (Fig. 2e, f). The rifts periodically form ~10 km inland of Chugunov Island (Fig. 2e), on the western section of the ice tongue, before being advected down-flow. But a more detailed analysis of how the rifts form is not possible because of the limited availability of satellite imagery in the 1970s and 80s. An analysis of the rifting pattern in 1974 and the iceberg formed in 1984 indicates that the iceberg calved from R7 (Fig. 2e, f). In contrast, on both the grounded iceberg observed in 1962 (Fig. 2d), which likely calved in the 1940s, and on the present day calving cycle (1984-present; Fig. 2g), similar rifting patterns are not observed.

3.2 Ice Speed

We observed widespread increases in ice speed across the entire Denman system between 1972-74 and 2016-17, with an overall acceleration of $19 \pm 5\%$ up to 50 km inland of the grounding line along the main trunk of the glacier (Fig. 3a). Specifically, at box *D*, 10 km inland of the grounding line, ice flow speed increased by $17 \pm 4\%$ between 1972-74 and 2016-17 (Fig. 3c). The largest rates of acceleration at box *D* took place between 1972-74 and 1989 when there was a speed-up of $11 \pm 5\%$. Between 1989 and 2016-17 there was a comparatively slower acceleration of $3 \pm 2\%$ (Fig. 3c). The advance rate of the ice-front followed a similar pattern, but accelerated at a much greater rate. The ice-front advance rate increased by $26 \pm 5\%$ between 1972-74 and 1989, whilst increasing at a slower rate between 1989 and 2018 ($9 \pm 1\%$; Fig. 3b). At box *S* on the neighbouring Scott Glacier, we observed a $17 \pm 10\%$ decrease in velocity between 1972-74 and 2016-17 (Fig. 3d). Similar decreases in ice flow speed are also observed near the shear margin between Shackleton Ice Shelf and Denman Glacier (Fig. 3a, e). The net result of an increase in velocity at Denman Glacier and decreases in velocity either side at the Shackleton Ice Shelf and Scott Glacier is a steepening of the velocity gradient at the shear margins (Fig. 3e). Ice speed profiles across Denman Glacier also indicate lateral migration of the shear margins of ~ 5 km in both the east and west directions through time (Fig. 3e).

3.3 Lateral migration of Denman's ice tongue

A comparison of satellite imagery between 1974 and 2002, when Denman's ice-front was in a similar location (e.g. Fig. 4b, c), reveals a lateral migration of its ice tongue and a change in the characteristics of the shear margins. North of Chugunov Island, towards the ice-front, we observe a bending and westward migration of the ice tongue in 2002, compared to its 1974 position (Fig. 4b, c). In 1974, the ice tongue was intensely shearing against Chugunov Island, as indicated by the heavily damaged shear margins (Fig. 4d). However, by 2002 the ice tongue made substantially less contact with Chugunov Island because this section of the ice tongue migrated westwards (Fig. 4d, e). South of Chugunov Island there was a greater divergence of flow between the Denman and Scott Glaciers in 2002 compared to 1974, resulting in a more damaged shear margin (Fig. 4d, e). On the western shear margin between Shackleton Ice Shelf and Denman's ice tongue there was no obvious change in structure between 1974 and 2002

(Fig. 4f, g). However, velocity profiles in this region show an eastward migration of the fast flowing ice tongue (Fig. 3e).

4. Numerical Modelling

4.1. Model Set-Up and Experimental Design

To help assess the possible causes of the acceleration of Denman Glacier since 1972 and the importance of changes we observe on Denman's ice tongue, we conduct diagnostic numerical modelling experiments using the finite-element, ice dynamics model Úa (Gudmundsson et al, 2012). Úa is used to solve the equations of the shallow-ice stream or 'shelfy-stream' approximation, (SSA , Cuffey & Paterson, 2010). This can be expressed for one horizontal dimension as:

$$2\partial_x \left(A^{-\frac{1}{n}} h (\partial_x u)^{\frac{1}{n}} \right) - G C^{-\frac{1}{m}} u^{\frac{1}{m}} = \rho g h \partial_x s + \frac{1}{2} g h^2 \partial_x \rho$$

Where A is the rate factor with its corresponding stress factor n , h is the vertical ice thickness, G is a grounding/flotation mask (1 for grounded ice, 0 for floating ice), C is the basal slipperiness with its corresponding stress exponent, m , ρ is the density of ice and g is the acceleration due to gravity. Previously the model has been used to understand rates and patterns of grounding line migration, and glacier responses to ice shelf buttressing and ice shelf thickness (e.g. Reese et al., 2018; Hill et al., 2019; Gudmundsson et al., 2019), and has been involved in several model intercomparison experiments (e.g. Pattyn et al., 2008; 2012; Leverman et al., 2020).

Modelled ice velocities are calculated on a finite-element grid using a vertically-integrated form of the momentum equations. The model domain consists of 93,371 elements with horizontal dimensions ranging from 250 m near the grounding line to 10 km further inland. Zero flow conditions are applied along the inland boundaries, chosen to match zero flow contours from observations. The relationship between creep and stress is assumed to follow Glen's flow law, using stress exponent $n=3$ and basal sliding is assumed to follow Weertman's sliding law, with its own stress exponent, $m=3$. Other modelling parameters related to ice rheology and basal conditions are the basal slipperiness, C , and the rate factor, A . We initialized the ice-flow model by changing both the ice rate factor A (Fig. S3b) and basal slipperiness C (Fig. S3c), using an inverse approach (Vogel, 2002), iterating until the surface velocities of the numerical model closely matched the 2009 measurements of ice flow (Fig. S3).

4.2. Perturbation Experiments

To ascertain the most likely causes of the observed acceleration for Denman Glacier we start from a baseline set-up representing the ice shelf in 2009 where both ice geometry and velocity are well known and compare to diagnostic simulations of reconstructed 1972 ice geometry. We chose 2009 for this baseline setup, because the calving front is in approximately the same position as in 1972 when our glacier observations start, thus ruling out any acceleration is response to a change in ice-front extent. We use the BedMachine (Morlighem et al., 2020) ice thickness, bathymetry and grounding line position and MEaSUREs ice velocities for 2009 (Mouginot et al., 2017) as inputs. The baseline simulation is then perturbed to test its response to a series of potential drivers that may be responsible for the observed changes in ice geometry since the 1970s. Specifically, we apply observation-based perturbations to test Denman's response to ice shelf thinning (i), grounding line retreat (ii) and the unpinning of Denman's ice tongue from Chugunov Island (iii), which are detailed below:

i. To represent ice shelf thinning since 1972, we take the mean annual rate of ice-thickness change from the 1994–2012 ice-shelf thickness change dataset (Paolo et. al., 2015) and scale it up to represent the total thickness change over the 37 years between 1972 and 2009, assuming that the 1994–2012 mean annual rate remains constant during this period. This thickness change is then applied to the 2009 ice geometry, modifying it to better represent the estimated 1972 ice thickness distribution of the Shackleton Ice Shelf, Denman ice tongue and Scott Glacier. Similar to the methodology of Gudmundsson et al. (2019), we only apply this thickness change to fully floating nodes, with no change of ice thickness for grounded ice and ice directly over the grounding line. The total thickness change applied is shown in Fig. S4. We refer to this perturbation as ‘ice shelf thinning’ because the majority of the floating portions of Denman’s ice tongue and Shackleton Ice Shelf have thinned since 1994, although some sections of Scott Glacier have actually thickened near its calving front (Fig. S4).

ii. In the Úa ice model, the grounding line position is not explicitly defined by the user but is instead a direct result of ice thickness, bedrock depth and the relative densities of ice and sea water. As such, the two ways to perturb a given grounding line are to either modify the ice thickness or the bedrock depth. Modifying the bedrock depth is the less disruptive approach because the resulting effect upon velocity is not biased by an imposed change in ice thickness at the grounding line effecting the regional ice velocity field due to flux conservation, in

addition to that caused by shifting the grounding line. Note that raising the bedrock to meet the underside of the ice shelf in this way is not a representation of any real earth processes, it is merely forcing the model to have the grounding line in a particular location, that than enables a diagnostic simulation. To represent grounding line retreat since 1972 we advanced Denman's grounding line from its position in the 2009 baseline set-up by 10 km to a possible 1972 position. This is achieved via raising the bedrock approximately ~20-30 m in the area shown in Fig. S4. We justify a 10 km retreat since 1972 based on the rate of grounding-line retreat observed between 1996 and 2017 (~5km; Brancato et al., 2020). For the newly grounded area, values of the bed slipperiness, C , are not generated in our model inversion, we therefore prescribe nearest-neighbour values to those at the grounding line in the model inversion.

iii. To represent the pinning of Denman's ice tongue against Chugunov Island in the 1972 observations (e.g. Fig. 4d, e), we artificially raise a small area of bedrock on the western edge of Chugunov Island (Fig. S4). Bed slipperiness was set to a value comparable to that immediately upstream of the grounding line. Note that, although past observations suggest that the ice in front of Chugunov Island has been damaged, possibly having an effect on its rate factor, A , we have decided to limit our investigation to the effect of pinning the ice on Chugunov Island without changing rate factor. To properly investigate the possible change in past rate factor we would need less spatially patchy 1972 velocities as well as an accurate understanding of past ice geometry (itself an unknown under investigation) to perform a model inversion for 1972 conditions.

These three adjustments are applied, both individually and in combination with each other, to the baseline model setup to produce seven different simulations (E1-7), summarized in Table 1, which perturb, respectively:

- E1. Ice shelf thinning.
- E2. Grounding line retreat
- E3. Ice shelf thinning and grounding line retreat
- E4. Unpinning from Chugunov Island
- E5. Ice shelf thinning and unpinning from Chugunov Island
- E6. Grounding line retreat and unpinning from Chugunov Island
- E7. Ice shelf thinning, grounding line retreat and the unpinning from Chugunov Island

Below we compare the instantaneous change in ice velocity arising from each perturbation experiment₁ to observed changes in velocity, and then use these comparisons to understand the relative importance of each process in contributing to Denman's behaviour over the past 50 years.

4.3. Model results

We show observed 2009 ice speed relative to each of the seven simulations_s which represent possible 1972 ice geometries (E1-7, Fig. 5b-h). In all cases, positive (red) values indicate areas where ice was flowing faster and negative (blue) values show areas where ice was flowing slower in 2009 relative to each 1972 simulation. Perturbing ice shelf thickness to represent ice shelf thinning since the 1970s results in higher velocities over both the grounded and floating portions of the Denman system (E1, Fig. 5b). However, the simulated acceleration on Denman's ice tongue (E1, Fig. 5b) is much larger than the observed acceleration, with the simulation showing a 50% acceleration in the area just downstream from the grounding line compared to the observed 20% acceleration between 1972 and 2009 (E1, Fig. 5**b**). Thus, it would appear that ice shelf thinning alone, is not consistent with the observed velocity changes on the Denman system. Perturbing the grounding line to account for a possible grounding line retreat since 1972 simulates comparable changes in ice flow speeds to observations near Denman's grounding line (E2, Fig. 5c), but it is unable to reproduce the observed increases in ice speed across Denman's ice tongue (E2, Fig. 5c). Thus, grounding line retreat, alone, is also unable to reproduce the observed pattern of velocity changes. Ice shelf thinning and retreating the grounding line results in very similar patterns in ice speed change (E3, Fig. 5d) to that of the grounding line retreat perturbation experiment (E2).

In isolation, simulating the unpinning of Denman's ice tongue from Chugunov Island has a very limited effect on ice flow speeds, with no change in speed near the grounding line and a very spatially limited change on the ice tongue (E4; Fig. 5e). However, when combining the unpinning perturbation with either ice shelf thinning (E5; Fig. 5f) or grounding line retreat (E6; Fig. 5g), it is clear that the unpinning from Chugunov Island causes an acceleration across Denman's ice tongue. For E5 this results in an even larger overestimate of ice speed change across Denman's ice tongue in comparison to experiment 1, which only perturbs ice shelf thickness. However, for experiment 6 the additional inclusion of the unpinning from Chugunov Island to grounding line retreat results in a simulated pattern of ice flow speed change very

similar to observations. Specifically the unpinning from Chugunov Island has caused an acceleration across the ice tongue that was not present in experiment 2. Combining all three perturbations (E7, Fig. 5h) produces changes in ice velocity that are most comparable to observations. Both the spatial pattern in ice speed change and the simulated ice speed within box *D* (Fig. 5i) are very similar to observations for both experiments, and the enhanced westward bending of the directional component of ice velocity in experiment E7 is more consistent with the observed westward bending of the ice tongue (e.g. Fig. 2b).

5. Discussion

5.1 Variation in Denman Glacier's calving cycle

Our calving cycle reconstruction, combined with historical observations (Cassin and Wilkes, 1858; Mawson, 1914; 1932) hint that Denman's multi-decadal high-magnitude calving cycle has remained broadly similar over the past 200 years. It periodically produces a large tabular iceberg, which then drifts ~60 km northwards before grounding on an offshore ridge, and typically remains in place for around 20 years before disintegrating/dispersing. However, more detailed observations and reconstructions of its past three calving events have shown that there are clear differences in both the size of icebergs produced and in ice tongue structure through time (Fig. 2). The large variation (50%) in both the size of iceberg produced and the location the ice front calved from indicates variability in its calving cycle.

Extending observational records for ice shelves that calve at irregular intervals, sizes or locations is especially important because it helps to distinguish between changes in glacier dynamics caused by longer-term variations in its calving cycle, and changes in glacier dynamics forced by climate. For example, there have been large variations in ice flow speed at the Brunt Ice Shelf over the past 50 years (Gudmundsson et al., 2017), but these large variations can be explained by internal processes following interactions with local pinning points during the ice shelf's calving cycle (Gudmundsson et al., 2017). In contrast, the widespread acceleration of outlet glaciers in the Amundsen Sea sector (Mouginot et al., 2014) is linked to enhanced intrusions of warm ocean water increasing basal melt rates (e.g. (Thoma et al., 2008; Jenkins et al., 2018), leading to ice shelf thinning (Paolo et al., 2015) and grounding line retreat (Rignot et al., 2011a). Thus, in the following section we discuss whether the observed speed-up of Denman since the 1970s (Fig. 3) is more closely linked to variations in its calving cycle

(e.g. Brunt Ice Shelf) or if it has been driven by climate and ocean forcing (e.g. Amundsen Sea).

5.2 What has caused Denman Glacier's acceleration since the 1970s?

We observe a spatially widespread acceleration of both Denman's floating and grounded ice. This is characterised by a $17 \pm 4\%$ increase in ice flow speed near the grounding line between 1972 and 2017 (Fig. 3c) and a $36 \pm 5\%$ acceleration in ice-front advance rate from 1972-2017, or $30 \pm 5\%$ increase in ice-front advance rate between 1962 and 2017 (Fig. 3b). Our estimates of the acceleration in ice front advance rate are of a comparable magnitude to the 36% acceleration of the ice tongue between 1957 and 2017, based on averaged point estimates across the ice tongue from repeat aerial surveys (Dolgushin, 1966; Rignot et al., 2019). Taken together, this suggests a limited change in ice tongue speed between 1957 and 1972, before a rapid acceleration between 1972 and 2017. However, the rate of acceleration throughout this period has not been constant (Fig. 3b, c). Between 1972 to 1990, observations indicate that ice accelerated $26 \pm 5\%$ on the ice tongue (Fig. 3b) and $11 \pm 5\%$ at the grounding line (Fig. 3c) in comparison to more limited accelerations of $9 \pm 1\%$ and $3 \pm 2\%$, respectively, between 1990-2017. When comparing these observations against our numerical modelling experiments we find that a combination of grounding line retreat, changes in ice shelf thickness and the unpinning of ice from Chugunov Island (Fig. 5h) are all required to explain an acceleration of a comparable magnitude and spatial pattern across the Denman system.

Averaged basal melt rates across the Shackleton/Denman system are comparable to the Getz Ice Shelf (Depoorter et al., 2013; Rignot et al., 2013). Close to Denman's deep grounding line, melt rates have been estimated at 45 m yr^{-1} (Brancato et al., 2020), suggesting the presence of modified Circumpolar Deep Water in the ice shelf cavity. At nearby Totten Glacier (Fig. 1a), wind-driven periodic intrusions of warm water flood the continental shelf and cause increased basal melt rates (Rintoul et al., 2016; Greene et al., 2017) and grounding line retreat (Li et al., 2015). It is possible that a similar process may be responsible for some of the observed changes at Denman Glacier. Hydrographic data collected from the Marine Mammals Exploring the Oceans Pole to Pole consortium (Treasure et al., 2017) show water temperatures of -1.31 to -0.26°C at depths between 550 and 850 m on the continental shelf in front of Denman (Brancato et al., 2020). Thus, whilst not confirmed, there is clear potential for warm water to reach Denman's grounding zone and enhance melt rates.

Recent observations of grounding line migration at Denman have shown a 5 km retreat along its western flank between 1996 and 2017 (Brancato et al., 2020). However, over this time period there was a limited change in the speed of Denman (2001-2017; $3 \pm 2\%$ acceleration; Fig. 3c) and our time series indicates that the acceleration initiated earlier, at some point between 1972 and 1990 (Fig. 3c). Reconstructions of the bed topography near the grounding line of Denman Glacier show that the western flank of Denman's grounding line was resting on a retrograde slope in 1996, a few kilometres behind a topographic ridge (Brancato et al., 2020). One possibility is that Denman's grounding line retreat initiated much earlier at some point in the 1970s in response to increased ocean temperatures enhancing melting of the ice tongue base. This initial grounding line retreat and possible ocean-induced ice tongue thinning may have caused the initial rapid acceleration between 1972 and 1990, before continuing at a slower rate. However, our numerical modelling shows that whilst the combination of the retreat of Denman's grounding line and ice tongue thinning can produce a similar magnitude of acceleration near the grounding line to observations (E3; Fig. 5d), these modelled processes cannot explain the widespread acceleration across the ice tongue (e.g. E4; Fig. 5e).

In order to simulate a comparable spatial acceleration across both Denman's grounded and floating ice to observations, the un-pinning of ice from Chugunov Island following Denman's last calving event in 1984 is required (e.g. E6 & 7; Fig. 5g, 5h). In isolation, the reduction in contact with Chugunov Island has had no effect on ice flow speeds at both Denman's grounding line and ice tongue (E4; Fig. 5e). However, when combined with grounding line retreat and ice tongue thinning, the spatial pattern of simulated ice speed change across the ice tongue more closely resemble observations (E6 & 7; Fig. 5g, 5h). Specifically, the unpinning of the ice tongue from Chugunov Island has caused an acceleration across much of Denman's ice tongue. The most likely explanation as to why the unpinning from Chugunov Island only influences ice speed patterns in combination with ice tongue thinning and grounding line retreat, and not in isolation, is that ice tongue thinning and grounding line retreat have caused a change in the direction of flow of the ice tongue since the 1970s. In all simulations that perturb either ice tongue thickness or retreat the grounding line (Fig. 5b, c, e, f, g, h), there is a clear westward bending in ice flow direction near Chugunov Island which results in a reduction in contact between the ice tongue and Chugunov Island. This is consistent with observations that show a distinctive westward bending of Denman's ice tongue since the 1970s (Fig. 2b). These findings therefore suggest that the reduction in contact with Chugunov Island following Denman's calving event in 1984 caused an instantaneous acceleration across large sections of its ice

tongue, meaning that this calving event has had a direct impact on the spatial pattern of acceleration observed between 1972 and 2017. However, because of the westward bending of Denman's ice tongue during its re-advance following its 1984 calving event, the ice tongue now makes limited contact with Chugunov Island (e.g. Fig. 4e) and has a very limited effect on ice flow speeds (e.g. E4; Fig. 5e).

The acceleration of Denman's ice tongue following its last major calving event in 1984 may have also caused a series of positive feedbacks resulting in further acceleration. We observe a steepening of the velocity gradient across Denman's shear margins and a pattern of the acceleration of the dominant Denman ice tongue and slowdown of the neighbouring Shackleton Ice Shelf and Scott Glacier (Fig. 3a). We also observe the lateral migration of the shear margins at sub-decadal timescales (Fig. 3e). These distinctive patterns in ice speed change are very similar to those reported at the Stamcomb-Wills Ice Shelf (Humbert et al., 2009) and between the Thwaites Ice Tongue and Eastern Ice Shelf (Mouginot et al., 2014; Miles et al., 2020), and are symptomatic of a weakening of shear margins. Therefore, we suggest that at Denman, after the initial acceleration following the reduction in contact with Chugunov Island, the shear margins may have weakened causing further acceleration. We do not include this process in our numerical experiments, and it may explain the divergence between observations and simulated ice speed change in the neighbouring Shackleton Ice Shelf and Scott Glacier (Fig. 3a; Fig. 5).

Overall, our observations and numerical simulations suggest that the cause of Denman's acceleration since the 1970s is complex and likely reflects a combination of processes linked to the ocean and a reconfiguration of Denman's ice tongue. One possibility is that the acceleration of ice across Denman's grounding line has almost entirely been driven by warm ocean forcing driving grounding line retreat and ice tongue thinning, with the unpinning of Denman's ice tongue from Chugunov Island only causing a localised acceleration across floating ice. An alternative explanation is that warm ocean forcing has caused ice tongue thinning and grounding line retreat, but the acceleration behind the grounding line has been enhanced through time by changes in ice tongue configuration. Either way, our results highlight that both oceanic processes and the changes in ice tongue structure associated with Denman's calving event have been important in causing Denman's observed acceleration.

5.3 Future evolution of Denman Glacier

In the short-term, an important factor in the evolution of the wider Denman/Shackleton system is Denman's next calving event. Whilst our observations do not suggest that a calving event is imminent (next 1-2 years), our calving cycle reconstruction indicates that a calving event at some point in the 2020s is highly likely. Because the calving cycle of Denman Glacier has demonstrated some variability in the past (e.g. Fig. 2), the precise geometry of its ice tongue after this calving event cannot be accurately predicted. In particular, it is unclear how Denman's ice tongue will realign in relation to Chugunov Island following its next calving event. For example, if following Denman's next calving event the direction of ice flow shifts eastwards to a similar configuration to the 1970s and the ice tongue makes contact with Chugunov Island, the increased resistance could slowdown Denman's ice tongue for the duration of its calving cycle, but it is unclear if any slowdown could propagate to the grounding line. Thus, this calving event may have important implications for the evolution of the Denman/Shackleton system for multiple decades because it could influence both ice flow speed and direction.

In the medium-term (next 50 years) atmospheric warming could also have a direct impact on the stability of the Denman/Shackleton system. Following the collapse of Larsen B in 2002, Shackleton is now the most northerly major ice shelf remaining in Antarctica, with most of the ice shelf lying outside the Antarctic Circle. Numerous surface meltwater features have been repeatedly reported on its surface (Kingslake et al., 2017; Stokes et al., 2019; Arthur et al., 2020). There is no evidence that these features currently have a detrimental impact on its stability, but there is a possibility that projected increases in surface melt (Trusel et al., 2015) could increase the ice shelves vulnerability to meltwater-induced hydrofracturing.

6. Conclusion

We have reconstructed Denman Glacier's calving cycle to show that its previous two calving events (~1940s and 1984) have varied in size by 50% and there have been clear differences in ice tongue structure, with a notable unpinning from Chugunov Island following the 1984 calving event. We also observe a long-term acceleration of Denman Glacier across both grounded and floating sections of ice, with both the ice front advance rate and ice near the grounding line accelerating by $36 \pm 5\%$ and $17 \pm 4\%$, respectively, between 1972 and 2017. We show that in order to simulate a post-1972 acceleration that is comparable with observations, its grounding line must have retreated since the 1970s. We also highlight the importance of the

reconfiguration of the Denman ice tongue system in determining the spatial pattern of acceleration observed.

The recent changes in the Denman system are important because Denman's grounding line currently rests on a retrograde slope which extends 50 km into its basin (Morlighem et al., 2020; Brancato et al., 2020), suggesting clear potential for marine ice sheet instability. Given the large catchment size, it has potential to make globally significant contributions to mean sea level rise in the coming decades (1.49 m; Morlighem et al., 2020). Crucial to assessing the magnitude of any future sea level contributions is improving our understanding of regional oceanography, and determining whether the observed changes at Denman are the consequence of a longer-term ocean warming. This is in addition to monitoring and understanding the potential impact of any future changes in the complex Shackleton/Denman ice shelf system.

Acknowledgements

This work was funded by the Natural Environment Research Council (grant number: NE/R000824/1). Landsat and the declassified historical imagery from 1962 is freely available and can be downloaded via Earth Explorer (<https://earthexplorer.usgs.gov/>). COSI-Corr is available at http://www.tectonics.caltech.edu/slip_history/spot_coseis/download_software.html. The source code for Úa is available at <https://doi.org/10.5281/zenodo.3706624>. MEaSUREs annual ice velocity maps are available at <https://doi.org/10.5067/9T4EPQXTJYW9>. The historical ice velocity, ice front shapefiles and model code will be uploaded to the UK Polar Data Centre. We also acknowledge the use of imagery from the NASA worldview application (<https://worldview.earthdata.nasa.gov/>), part of the NASA Earth Observing System Data and Information System (EOSDIS). We also thank Eric Rignot for providing digitized estimates of ice flow speed across parts of Denman's ice tongue, based on the mapped estimates of Dolgushin et al. (1966). We would like to thank Chad Greene and two anonymous reviewers, along with the editor – Bert Wouters – for providing constructive comments which led to the improvement of this manuscript.

References

- Aitken, A. R. A., Roberts, J. L., van Ommen, T. D., Young, D. A., Golledge, N. R., Greenbaum, J. S., Blankenship, D. D., and Siegert, M. J.: Repeated large-scale retreat and advance of Totten Glacier indicated by inland bed erosion, *Nature*, 533, 385–+, 2016.
- Arthur, J. F., Stokes, C. R., Jamieson, S. S. R., Carr, J. R., and Leeson, A. A.: Distribution and seasonal evolution of supraglacial lakes on Shackleton Ice Shelf, East Antarctica, *The Cryosphere Discuss.*, <https://doi.org/10.5194/tc-2020-101>, in review, 2020.
- Brancato, V., Rignot, E., Milillo, P., Morlighem, M., Mouginot, J., An, L., Scheuchl, B., Jeong, S., Rizzoli, P., Bueso Bello, J. L., and Prats-Iraola, P.: Grounding line retreat of Denman Glacier, East Antarctica, measured with COSMO-SkyMed radar interferometry data, *Geophys Res Lett*, n/a, e2019GL086291.
- Burke, K. D., Williams, J. W., Chandler, M. A., Haywood, A. M., Lunt, D. J., and Otto-Bliesner, B. L.: Pliocene and Eocene provide best analogs for near-future climates, *P Natl Acad Sci USA*, 115, 13288–13293, 2018.
- Cassin, J. and Wilkes, C. United States Exploring Expedition: During the Years 1838, 1839, 1840, 1841, 1842, Under the Command of Charles Wilkes, USN. Mammalogy and Ornithology. JB Lippincott & Company, 1858.
- Cuffey, K.M. and W.S.B. Paterson. The physics of glaciers. Fourth edition. Amsterdam, etc., Academic Press. 704pp. ISBN-10: 0-123694-61-2, ISBN-13: 978-0-123-69461-4, hardback, £60.99/€71.95/US\$99.95. *Journal of Glaciology*, 57(202), 383–384. doi:10.3189/002214311796405906, 2010.
- DeConto, R. M. and Pollard, D.: Contribution of Antarctica to past and future sea-level rise, *Nature*, 531, 591–+, 2016.
- Depoorter, M. A., Bamber, J. L., Griggs, J. A., Lenaerts, J. T. M., Ligtenberg, S. R. M., van den Broeke, M. R., and Moholdt, G.: Calving fluxes and basal melt rates of Antarctic ice shelves, *Nature*, 502, 89–+, 2013.
- Dolgushin, L. D. New data on the rates of movement of Antarctic glaciers. *Soviet Antarctic Expedition Information Bulletin* 55 (1966): 41–42.
- Flament, T. and Remy, F.: Dynamic thinning of Antarctic glaciers from along-track repeat radar altimetry, *J Glaciol*, 58, 830–840, 2012.
- Gardner, A. S., Moholdt, G., Scambos, T., Fahnestock, M., Ligtenberg, S., van den Broeke, M., and Nilsson, J.: Increased West Antarctic and unchanged East Antarctic ice discharge over the last 7 years, *Cryosphere*, 12, 521–547, 2018.
- Gasson, E., DeConto, R., and Pollard, D.: Antarctic bedrock topography uncertainty and ice sheet stability, *Geophys Res Lett*, 42, 5372–5377, 2015.

542 Golledge, N. R., Kowalewski, D. E., Naish, T. R., Levy, R. H., Fogwill, C. J., and Gasson, E.
 543 G. W.: The multi-millennial Antarctic commitment to future sea-level rise, *Nature*, 526,
 544 421–+, 2015.

545 Greenbaum, J. S., Blankenship, D. D., Young, D. A., Richter, T. G., Roberts, J. L., Aitken, A.
 546 R. A., Legresy, B., Schroeder, D. M., Warner, R. C., van Ommen, T. D., and Siegert, M. J.:
 547 Ocean access to a cavity beneath Totten Glacier in East Antarctica, *Nat Geosci*, 8, 294–298,
 548 2015.

549 Greene, C. A., Blankenship, D. D., Gwyther, D. E., Silvano, A., and van Wijk, E.: Wind causes
 550 Totten Ice Shelf melt and acceleration, *Science Advances*, 3, 2017.

551 Gudmundsson, G. H.: Ice-shelf buttressing and the stability of marine ice sheets, *Cryosphere*,
 552 7, 647–655, 2013.

553 Gudmundsson, G. H., de Rydt, J., and Nagler, T.: Five decades of strong temporal variability
 554 in the flow of Brunt Ice Shelf, Antarctica, *J Glaciol*, 63, 164–175, 2017.

555 Gudmundsson, G. H., Krug, J., Durand, G., Favier, L., and Gagliardini, O.: The stability of
 556 grounding lines on retrograde slopes, *Cryosphere*, 6, 1497–1505, 2012.

557 Gudmundsson, G. H., Paolo, F. S., Adusumilli, S., & Fricker, H. A. Instantaneous Antarctic
 558 ice- sheet mass loss driven by thinning ice shelves. *Geophysical Research Letters*, 46,
 559 13903– 13909. <https://doi.org/10.1029/2019GL085027>, 2019

560 Helm, V., Humbert, A., and Miller, H.: Elevation and elevation change of Greenland and
 561 Antarctica derived from CryoSat-2, *Cryosphere*, 8, 1539–1559, 2014.

562 Hill, E. A., Gudmundsson, G. H., Carr, J. R., and Stokes, C. R.: Velocity response of Petermann
 563 Glacier, northwest Greenland, to past and future calving events, *The Cryosphere*, 12, 3907–
 564 3921, <https://doi.org/10.5194/tc-12-3907-2018>, 2018.

565 Humbert, A., Kleiner, T., Mohrholz, C. O., Oelke, C., Greve, R., and Lange, M. A.: A
 566 comparative modeling study of the Brunt Ice Shelf/Stamcomb-Wills Ice Tongue system, East
 567 Antarctica, *J Glaciol*, 55, 53–65, 2009.

568 Jenkins, A., Shoosmith, D., Dutrieux, P., Jacobs, S., Kim, T. W., Lee, S. H., Ha, H. K., and
 569 Stammerjohn, S.: West Antarctic Ice Sheet retreat in the Amundsen Sea driven by decadal
 570 oceanic variability, *Nat Geosci*, 11, 733–+, 2018.

571 King, M. A., Bingham, R. J., Moore, P., Whitehouse, P. L., Bentley, M. J., and Milne, G. A.:
 572 Lower satellite-gravimetry estimates of Antarctic sea-level contribution, *Nature*, 491, 586–
 573 +, 2012.

574 Kingslake, J., Ely, J. C., Das, I., and Bell, R. E.: Widespread movement of meltwater onto and
 575 across Antarctic ice shelves, *Nature*, 544, 349–+, 2017.

576 Lea, J. M.: The Google Earth Engine Digitisation Tool (GEEDiT) and the Margin change
577 Quantification Tool (MaQiT) - simple tools for the rapid mapping and quantification of
578 changing Earth surface margins, *Earth Surf Dynam*, 6, 551-561, 2018.

579 Leprince, S., Ayoub, F., Klinger, Y., and Avouac, J. P.: Co-Registration of Optically Sensed
580 Images and Correlation (COSI-Corr): an operational methodology for ground deformation
581 measurements, *Igarss: 2007 Ieee International Geoscience and Remote Sensing*
582 *Symposium*, Vols 1-12, doi: 10.1109/Igarss.2007.4423207, 2007. 1943-+, 2007.

583 Levermann, A., Winkelmann, R., Albrecht, T., Goelzer, H., Golledge, N. R., Greve, R.,
584 Huybrechts, P., Jordan, J., Leguy, G., Martin, D., Morlighem, M., Pattyn, F., Pollard, D.,
585 Quiquet, A., Rodehacke, C., Seroussi, H., Sutter, J., Zhang, T., Van Breedam, J., Calov, R.,
586 DeConto, R., Dumas, C., Garbe, J., Gudmundsson, G. H., Hoffman, M. J., Humbert, A.,
587 Kleiner, T., Lipscomb, W. H., Meinshausen, M., Ng, E., Nowicki, S. M. J., Perego, M.,
588 Price, S. F., Saito, F., Schlegel, N.-J., Sun, S., and van de Wal, R. S. W.: Projecting
589 Antarctica's contribution to future sea level rise from basal ice shelf melt using linear
590 response functions of 16 ice sheet models (LARMIP-2), *Earth Syst. Dynam.*, 11, 35–76,
591 <https://doi.org/10.5194/esd-11-35-2020>, 2020.

592 Li, X., Rignot, E., Morlighem, M., Mouginot, J., and Scheuchl, B.: Grounding line retreat of
593 Totten Glacier, East Antarctica, 1996 to 2013, *Geophys Res Lett*, 42, 8049-8056, 2015.

594 Li, X., Rignot, E., and Mouginot, J.: Ice flow dynamics and mass loss of Totten Glacier, East
595 Antarctica, from 1989 to 2015, *Geophys Res Lett*, 43, 6366-6373, 2016.

596 [Lovell, A., Stokes, C., & Jamieson, S. Sub-decadal variations in outlet glacier terminus](#)
597 [positions in Victoria Land, Oates Land and George V Land, East Antarctica \(1972–2013\).](#)
598 [Antarctic Science, 29\(5\), 468-483. 2017.](#)

599 Mawson, D., *The Home of the Blizzard*, Heinemann, London, 1915.

600 Mawson, Douglas. "The BANZ Antarctic Research Expedition, 1929-31." *The Geographical*
601 *Journal* 80.2 (1932): 101-126.

602 Miles, B. W. J., Stokes, C. R., and Jamieson, S. S. R.: Pan-ice-sheet glacier terminus change
603 in East Antarctica reveals sensitivity of Wilkes Land to sea-ice changes, *Science Advances*,
604 2, 2016.

605 Miles, B. W. J., Stokes, C. R., and Jamieson, S. S. R.: Velocity increases at Cook Glacier, East
606 Antarctica, linked to ice shelf loss and a subglacial flood event, *Cryosphere*, 12, 3123-3136,
607 2018.

608 Miles, B. W. J., Stokes, C. R., Jenkins, A., Jordan, J. R., Jamieson, S. S. R., and Gudmundsson,
609 G. H.: Intermittent structural weakening and acceleration of the Thwaites Glacier Tongue
610 between 2000 and 2018, *J Glaciol*, 66, 485-495, 2020.

611 Miles, B. W. J., Stokes, C. R., Vieli, A., and Cox, N. J.: Rapid, climate-driven changes in outlet
612 glaciers on the Pacific coast of East Antarctica, *Nature*, 500, 563-+, 2013.

613 Mohajerani, Y., Velicogna, I., and Rignot, E.: Evaluation of Regional Climate Models Using
614 Regionally Optimized GRACE Mascons in the Amery and Getz Ice Shelves Basins,
615 Antarctica, *Geophys Res Lett*, 46, 13883-13891, 2019.

616 Moon, T. and Joughin, I.: Changes in ice front position on Greenland's outlet glaciers from
617 1992 to 2007, *J Geophys Res-Earth*, 113, 2008.

618 Morlighem, M., Rignot, E., Binder, T., Blankenship, D., Drews, R., Eagles, G., Eisen, O.,
619 Ferraccioli, F., Forsberg, R., Fretwell, P., Goel, V., Greenbaum, J. S., Gudmundsson, H.,
620 Guo, J. X., Helm, V., Hofstede, C., Howat, I., Humbert, A., Jokat, W., Karlsson, N. B., Lee,
621 W. S., Matsuoka, K., Millan, R., Mouginot, J., Paden, J., Pattyn, F., Roberts, J., Rosier, S.,
622 Ruppel, A., Seroussi, H., Smith, E. C., Steinhage, D., Sun, B., van den Broeke, M. R., van
623 Ommen, T. D., van Wessem, M., and Young, D. A.: Deep glacial troughs and stabilizing
624 ridges unveiled beneath the margins of the Antarctic ice sheet, *Nat Geosci*, 13, 132-+, 2020.

625 Mouginot, J., Rignot, E., and Scheuchl, B.: Sustained increase in ice discharge from the
626 Amundsen Sea Embayment, West Antarctica, from 1973 to 2013, *Geophys Res Lett*, 41,
627 1576-1584, 2014.

628 Mouginot, J., Rignot, E., Scheuchl, B., and Millan, R.: Comprehensive Annual Ice Sheet
629 Velocity Mapping Using Landsat-8, Sentinel-1, and RADARSAT-2 Data, *Remote Sens-
630 Basel*, 9, 2017.

631 Paolo, F. S., Fricker, H. A., and Padman, L.: Volume loss from Antarctic ice shelves is
632 accelerating, *Science*, doi: 10.1126/science.aaa0940, 2015. 2015.

633 Pritchard, H. D., Arthern, R. J., Vaughan, D. G., and Edwards, L. A.: Extensive dynamic
634 thinning on the margins of the Greenland and Antarctic ice sheets, *Nature*, 461, 971-975,
635 2009.

636 Pattyn, F., Perichon, L., Aschwanden, A., Breuer, B., de Smedt, B., Gagliardini, O.,
637 Gudmundsson, G. H., Hindmarsh, R. C. A., Hubbard, A., Johnson, J. V., Kleiner, T.,
638 Konovalov, Y., Martin, C., Payne, A. J., Pollard, D., Price, S., Rückamp, M., Saito, F.,
639 Souček, O., Sugiyama, S., and Zwinger, T.: Benchmark experiments for higher-order and
640 full-Stokes ice sheet models (ISMIP-HOM), *The Cryosphere*, 2, 95–108,
641 <https://doi.org/10.5194/tc-2-95-2008>, 2008.

642 Pattyn, F., Schoof, C., Perichon, L., Hindmarsh, R. C. A., Bueler, E., de Fleurian, B., Durand,
643 G., Gagliardini, O., Gladstone, R., Goldberg, D., Gudmundsson, G. H., Huybrechts, P., Lee,
644 V., Nick, F. M., Payne, A. J., Pollard, D., Rybak, O., Saito, F., and Vieli, A.: Results of the
645 Marine Ice Sheet Model Intercomparison Project, MISIP, *The Cryosphere*, 6, 573–588,
646 <https://doi.org/10.5194/tc-6-573-2012>, 2012.

647 Rignot, E., Jacobs, S., Mouginot, J., and Scheuchl, B.: Ice-Shelf Melting Around Antarctica,
648 Science, 341, 266-270, 2013.

649 Rignot, E., Mouginot, J., and Scheuchl, B.: Antarctic grounding line mapping from differential
650 satellite radar interferometry, *Geophys Res Lett*, 38, 2011a.

651 Rignot, E., Mouginot, J., and Scheuchl, B.: Ice Flow of the Antarctic Ice Sheet, *Science*, 333,
652 1427-1430, 2011b.

653 Rignot, E., Mouginot, J., Scheuchl, B., van den Broeke, M., van Wessem, M. J., and
654 Morlighem, M.: Four decades of Antarctic Ice Sheet mass balance from 1979-2017, *P Natl*
655 *Acad Sci USA*, 116, 1095-1103, 2019.

656 Rintoul, S. R., Silvano, A., Pena-Molino, B., van Wijk, E., Rosenberg, M., Greenbaum, J. S.,
657 and Blankenship, D. D.: Ocean heat drives rapid basal melt of the Totten Ice Shelf, *Science*
658 *Advances*, 2, 2016.

659 Ritz, C., Edwards, T. L., Durand, G., Payne, A. J., Peyaud, V., and Hindmarsh, R. C. A.:
660 Potential sea-level rise from Antarctic ice-sheet instability constrained by observations,
661 *Nature*, 528, 115-+, 2015.

662 Scherer, R. P., DeConto, R. M., Pollard, D., and Alley, R. B.: Windblown Pliocene diatoms
663 and East Antarctic Ice Sheet retreat, *Nat Commun*, 7, 2016.

664 Scherler, D., Leprince, S., and Strecker, M. R.: Glacier-surface velocities in alpine terrain from
665 optical satellite imagery - Accuracy improvement and quality assessment, *Remote Sens*
666 *Environ*, 112, 3806-3819, 2008.

667 Schoof, C.: Ice sheet grounding line dynamics: Steady states, stability, and hysteresis, *J*
668 *Geophys Res-Earth*, 112, 2007.

669 Schröder, L., Horwath, M., Dietrich, R., and Helm, V.: Four decades of surface elevation
670 change of the Antarctic Ice Sheet from multi-mission satellite altimetry, *The Cryosphere*
671 *Discuss.*, 2018, 1-25, 2018.

672 Shen, Q., Wang, H. S., Shum, C. K., Jiang, L. M., Hsu, H. T., and Dong, J. L.: Recent high-
673 resolution Antarctic ice velocity maps reveal increased mass loss in Wilkes Land, East
674 Antarctica, *Sci Rep-Uk*, 8, 2018.

675 Stokes, C. R., Sanderson, J. E., Miles, B. W. J., Jamieson, S. S. R., and Leeson, A. A.:
676 Widespread distribution of supraglacial lakes around the margin of the East Antarctic Ice
677 Sheet. *Sci Rep* 9, 13823, 2019.

678 Thoma, M., Jenkins, A., Holland, D., and Jacobs, S.: Modelling Circumpolar Deep Water
679 intrusions on the Amundsen Sea continental shelf, Antarctica, *Geophys Res Lett*, 35, 2008.

680 Trusel, L. D., Frey, K. E., Das, S. B., Karnauskas, K. B., Munneke, P. K., van Meijgaard, E.,
681 and van den Broeke, M. R.: Divergent trajectories of Antarctic surface melt under two
682 twenty-first-century climate scenarios, *Nat Geosci*, 8, 927-U956, 2015.

683 Vogel, C. R. Computational methods for inverse problems. Vol. 23. Siam, 2002.

- Williams, T., van de Flierdt, T., Hemming, S. R., Chung, E., Roy, M., and Goldstein, S. L.:
Evidence for iceberg armadas from East Antarctica in the Southern Ocean during the late
Miocene and early Pliocene, *Earth Planet Sc Lett*, 290, 351-361, 2010.
- Young, D. A., Lindzey, L. E., Blankenship, D. D., Greenbaum, J. S., de Gorord, A. G., Kempf,
S. D., Roberts, J. L., Warner, R. C., Van Ommen, T., Siegert, M. J., and Le Meur, E.: Land-
ice elevation changes from photon-counting swath altimetry: first applications over the
Antarctic ice sheet, *J Glaciol*, 61, 17-28, 2015.
- Young, D. A., Wright, A. P., Roberts, J. L., Warner, R. C., Young, N. W., Greenbaum, J. S.,
Schroeder, D. M., Holt, J. W., Sugden, D. E., Blankenship, D. D., van Ommen, T. D., and
Siegert, M. J.: A dynamic early East Antarctic Ice Sheet suggested by ice-covered fjord
landscapes, *Nature*, 474, 72-75, 2011.
- Weertman J., Stability of the junction of an ice sheet and an ice shelf. *J. Glaciol.*, 13(67), 3–11,
1974.

Table 1: Summary of the perturbations included in each of our seven numerical modelling experiments

Experiment	Ice Shelf Thinning	Grounding Line Retreat	Unpinning from Chugunov Island
E1	✓		
E2		✓	
E3	✓	✓	
E4			✓
E5	✓		✓
E6		✓	✓
E7	✓	✓	✓

Figures

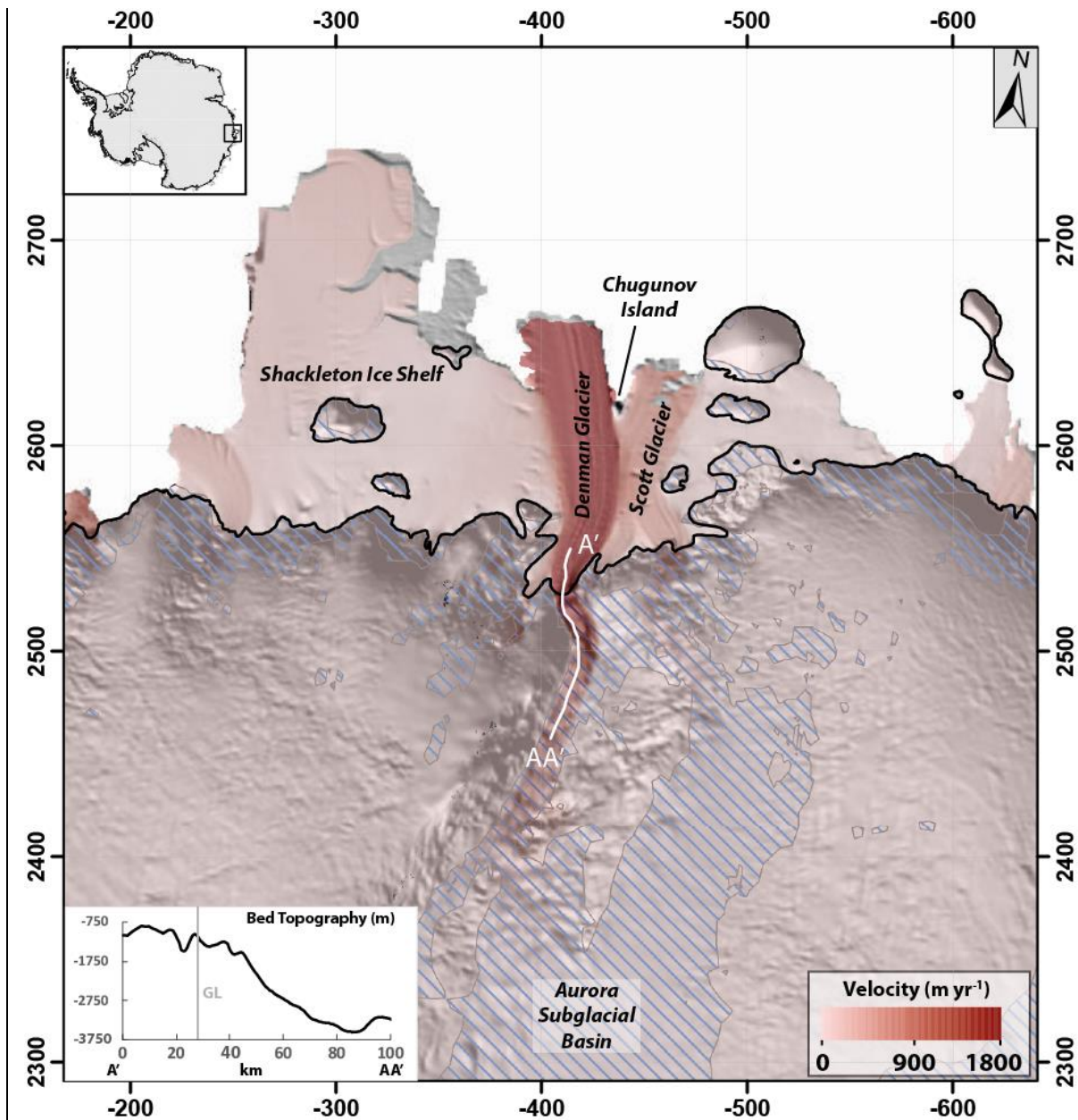


Figure 1: REMA mosaic (Howat et al., 2019) of the Denman Glacier and Shackleton Ice Shelf, note the numerous pinning points on the Shackleton Ice Shelf. The MEaSUREs velocity product is overlain (Rignot et al., 2011) and the grounding line product from Depoorter et al. (2013). The hatched blue lines represent regions where bedrock elevation below sea level, note how Denman Glacier drains the Aurora Subglacial Basin. A profile of bedrock elevation from BedMachine (Morligham et al., 2020) along the transect A'-AA' is located on the bottom left of the figure. Note the reverse bed slope. The coordinates are in polar stereographic (km).

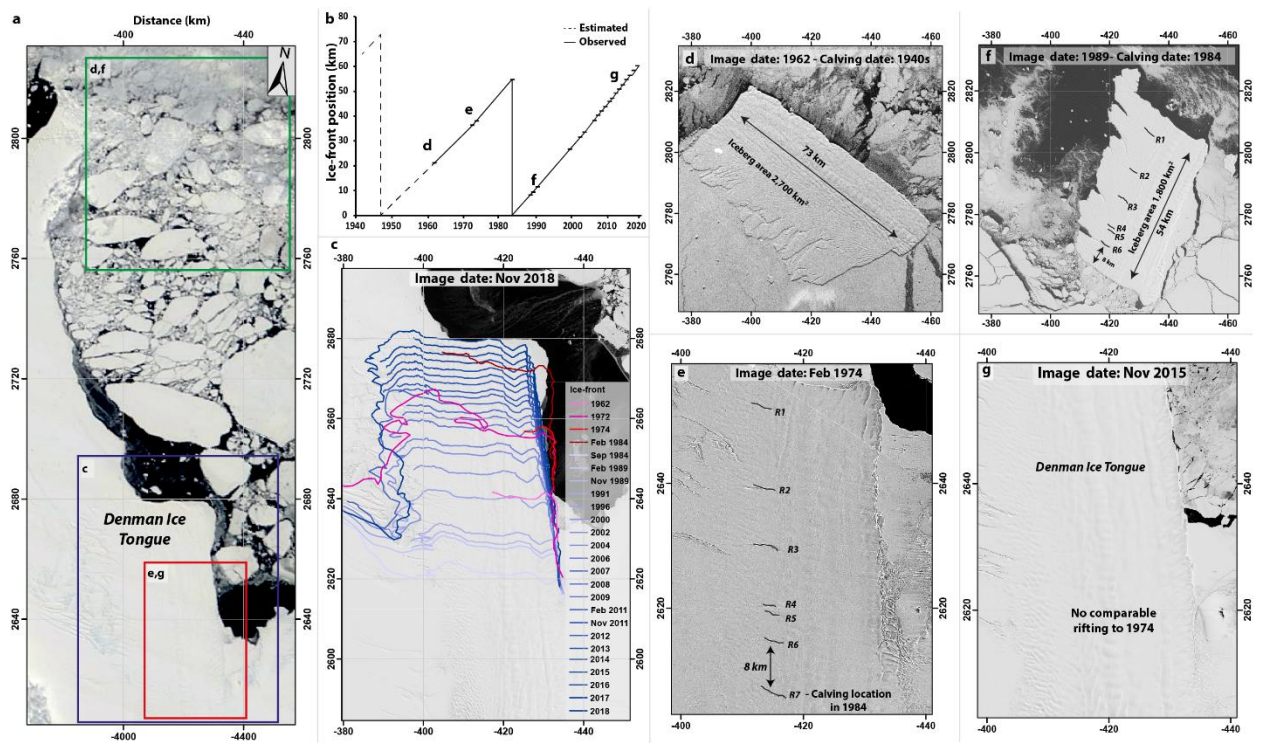


Figure 2: a) MODIS image from Worldview of the Denman ice tongue in November 2018 with the coloured boxes indicating the locations of panels c-g. b) Reconstructed calving cycle of Denman Glacier 1940-2018. c) Examples of ice-front mapping 1962-2018. Note the change in angle of the ice shelf between its present (light blue – dark blue lines) and previous (pink-red lines) calving cycle. d) ARGON image of a large tabular iceberg in 1962 which likely calved from Denman at some point in the 1940s. e) Landsat-1 image of the Denman ice tongue in 1972, note the pattern of rifting which is digitized in black for increased visibility and labelled R1-R7. f) Landsat-4 image of a large tabular iceberg which calved from Denman in 1984. Note the rifting pattern and the absence of R7, meaning R7 likely propagated during its calving event in 1984. g) Landsat-8 image of the Denman ice tongue in 2015. Note the absence of rifting. All Landsat images in this figure have been made available courtesy of the U.S. Geological Survey.

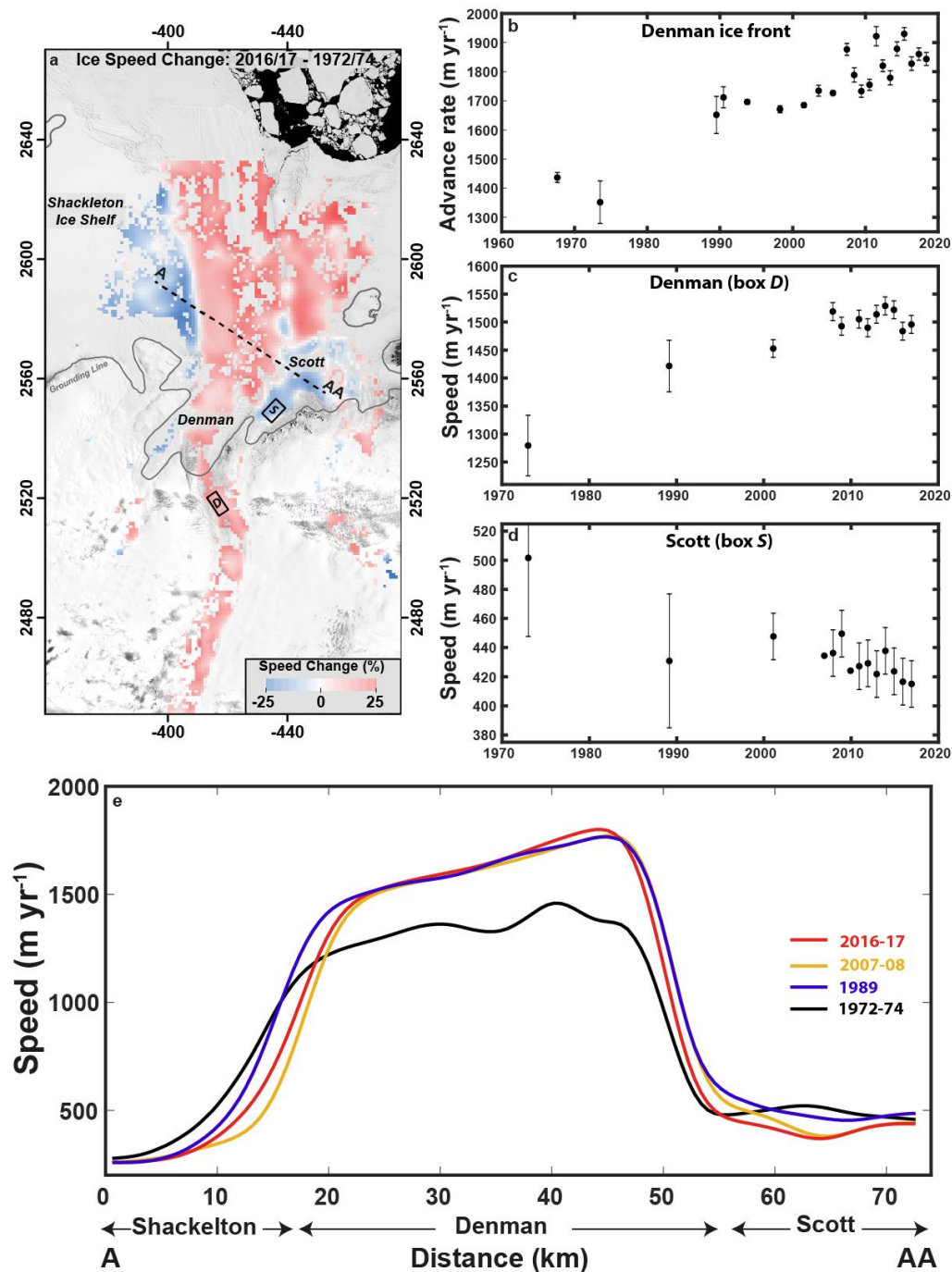


Figure 3: a) Percentage difference in ice speed between 2016-17 and 1972-74 overlain on a Landsat-8 image from November 2017 provided by the U.S. Geological Survey. Red indicates a relative increase in 2016-17 and blue a relative decrease in 2016-17. The grounding line is in grey (Depoorter et al., 2013) b) Time series of the advance rate of the Denman ice-front 1962-2018. c) Time series of mean ice speed from box D, 1972-2017) approximately 10 km behind the Denman grounding line. d) Time series of mean ice speed from box S, on Scott Glacier, 1972-2017. e) Ice speed profiles across the Shackleton-Denman-Scott system from 1972-74, 1989, 2007-08 and 2016-17. Note the lateral migration of the shear margins.

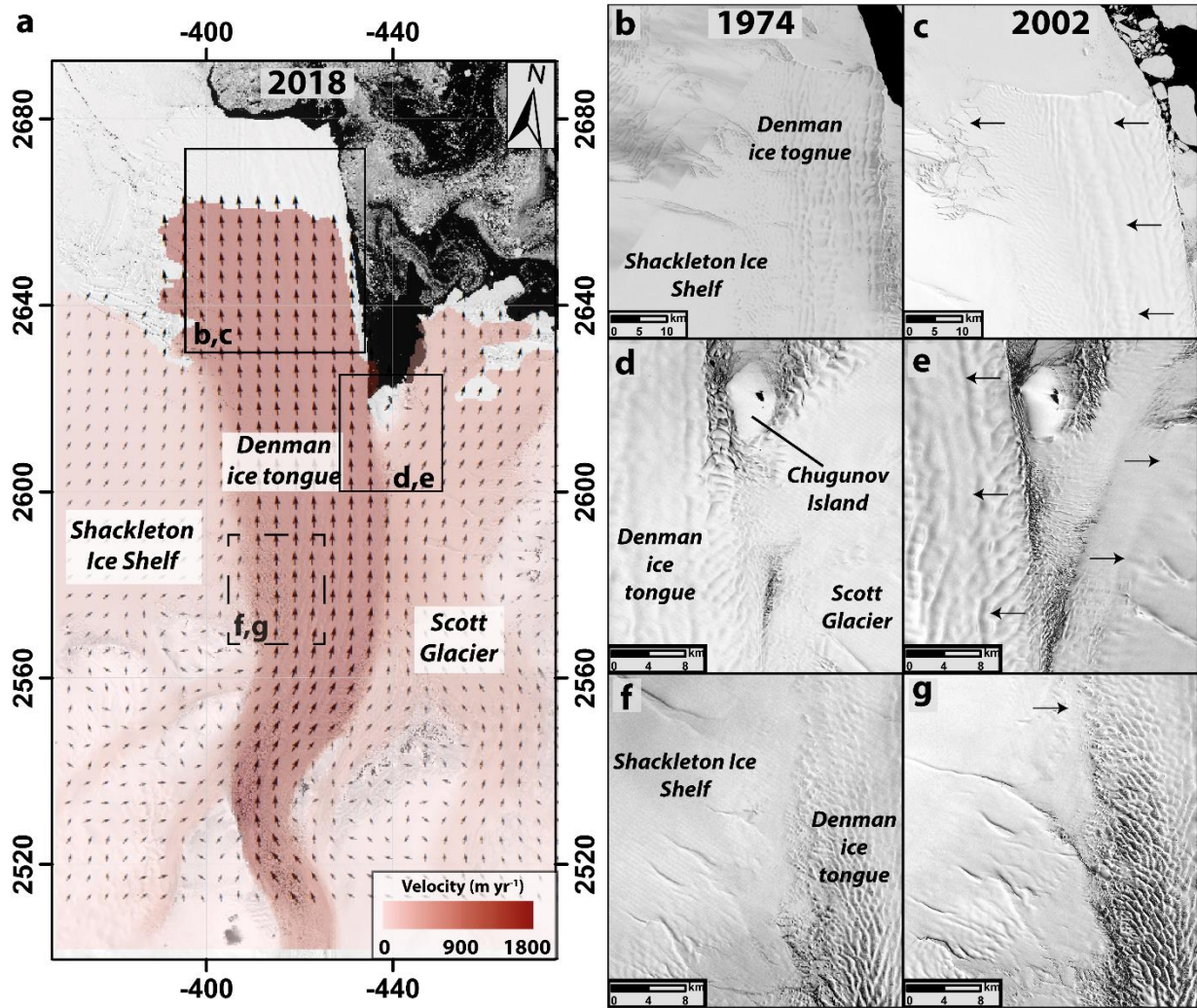


Figure 4: a) Landsat-8 image overlain with MEaSUREs velocity vectors (Rignot et al., 2011). b), d) and f) Close-up in examples of ice tongue structure and position from a Landsat-1 image in 1974. c), e) and g) Close-up in examples of ice tongue structure and position from a Landsat-7 image in 2002. In particular, note the reduction in contact between Denman Glacier and Chugunov Island between 1974 (d) and 2002 (e). The arrows on panels c,e and g represent to direction of migration of the Denman ice tongue since 1974. All Landsat images in this figure have been made available courtesy of the U.S. Geological Survey.

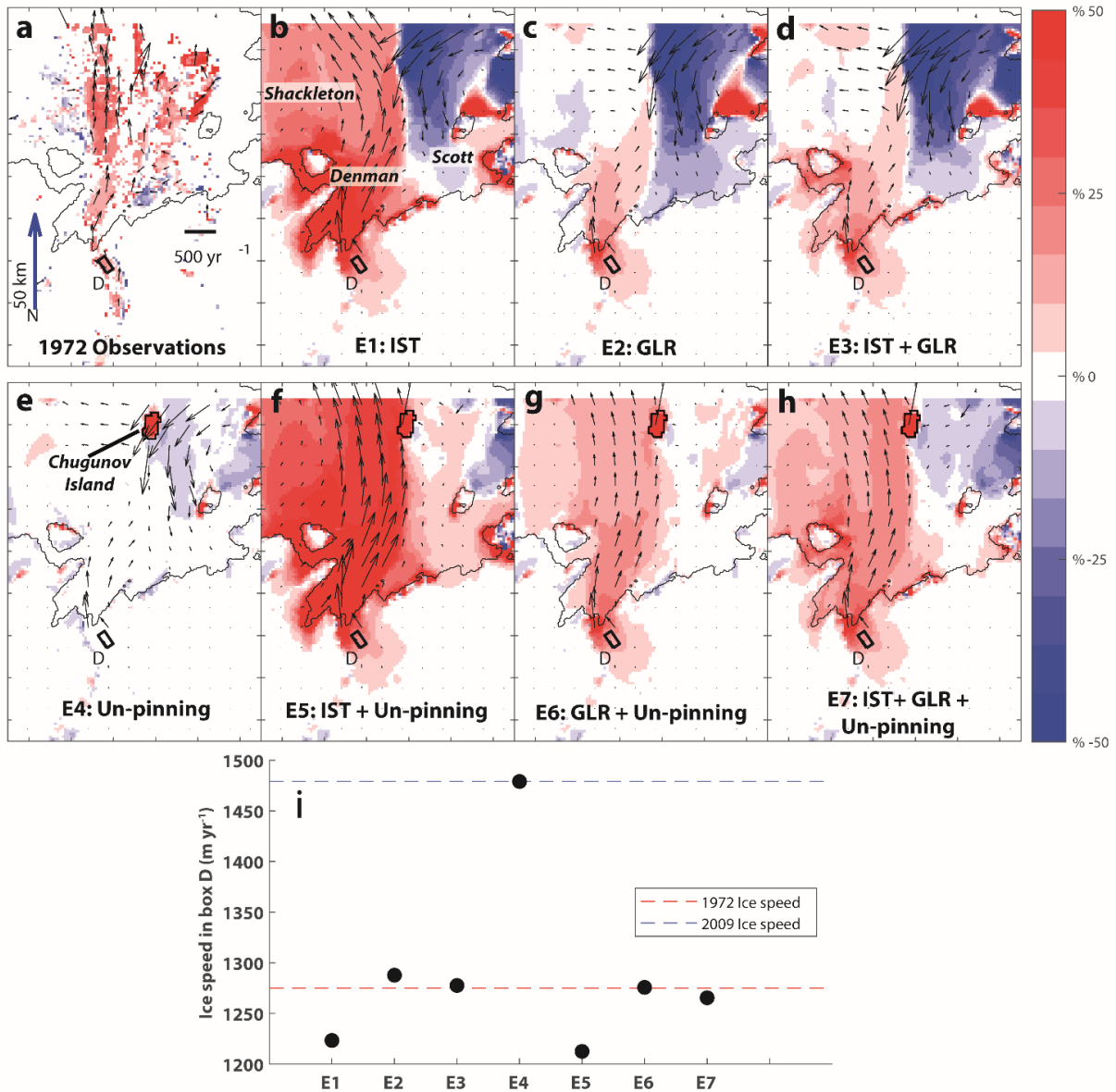


Figure 5 – The effect of varying ice geometry on ice flow: Ice velocity difference between 2009 observations and a) observations from 1972, and b)-h) seven experiments which perturb 2009 ice geometry to represent possible 1972 ice geometry configurations. In each experiment combinations of Ice shelf thinning (IST), Grounding line retreat (GLR) and the un-pinning from Chugunov Island are perturbed (See Table 1). Note that red indicates areas where ice is flowing faster in 2009 and blue indicates areas that are flowing slower with arrows showing the direction and magnitude of change when compared to the 1972 perturbations. I) Mean speed from box D in each experiment, the dotted red line represents observed mean speed from box D in 1972 and the blue line observed speed from 2009. E7 most closely matches the speed observed in box D, the spatial pattern of the observed acceleration and the westward bending of Denman’s ice tongue.